Pergamon

Journal of Structural Geology, Vol. 20, No. 9/10, pp. 1365 to 1393, 1998

0191-8141/98/$ - see front matter

PII: S0191-8141(98)00074-1

Granite ascent and emplacement during contractional deformation in convergent orogens

MICHAEL BROWN and GARY S. SOLAR

Laboratory for Crustal Petrology, Department of Geology, University of Maryland, College Park, MD 20742-4211, U.S.A., E-mail; mbrown@geol.umd.edu

(*Received* 1 *July* 1997; *accepted in revised form* 20 *April* 1998)

Abstract—Based on a case study in the Central Maine Belt of west-central Maine, U.S.A., it is proposed that crustal-scale shear zone systems provide an effective focussing mechanism for transfer of granite melt through the crust in convergent orogens. During contractional deformation, flow of melt in crustal materials at depths below the brittle–plastic transition is coupled with plastic deformation of these materials. The flow is driven by pressure gradients generated by buoyancy forces and tectonic stresses. Within the oblique-reverse Central Maine Belt shear zone system, stromatic migmatite and concordant to weakly discordant irregular granite sheets occur in zones of higher strain, which suggests percolative flow of melt to form the migmatite leucosomes and viscous flow of melt channelized in sheet-like bodies, possibly along fractures. Cyclic fluctuations of melt pressure may cause instantaneous changes in the effective permeability of the flow network if self-propagating melt-filled tensile and/or dilatant shear fractures are produced due to melt-enhanced embrittlement. Inhomogeneous migmatite and schlieric granite occur in zones of lower strain, which suggests migration of partially-molten material through these zones *en masse* by granular flow, and channelized flow of melt carrying entrained residue. Founded on the Central Maine Belt case study, we develop a model of melt extraction and ascent using the driving forces, stress conditions and crustal rheologies in convergent, especially transpressive orogens. Ascent of melt becomes inhibited with decreasing depth as the solidus is approached. For intermediate $a(H_2O)$ muscovite-dehydration melting, the water-saturated solidus occurs between 400 and 200 MPa, near the brittle–plastic transition during high-*T*–low-*P* metamorphism, where the balance of forces favors (sub-) horizontal fracture propagation. Emplacement of melt may be accommodated by ductile flow and/or stoping of wall rock, and inflation may be accommodated by lifting of the roof at shallower crustal levels and/or sinking of the pluton floor. The resultant plutons have (sub-) horizontal tabular geometries with floors that slope down to the ascent conduits. Although these plutons may have locally discordant relations with country rock structures, when viewed at the crustal-scale, granite ascent and emplacement in convergent orogens are syn-tectonic processes.

INTRODUCTION

Migration of granite melt is important in the evolution of the continents because it advects heat and mass from the lower to the upper crust, which in turn contributes to metamorphic activity in the upper crust and is responsible for chemical differentiation of the continents. In addition, the melt induces thermal and mechanical interactions during ascent and emplacement that affect the crustal response to stresses in the lithosphere. Many aspects of the extraction and transfer process remain poorly understood or controversial, however, including focussing the melt and the mechanism of ascent (Rubin, 1993a; Petford, 1996; Weinberg, 1996) and the relationship between ascent and active deformation in convergent orogens (e.g. Hollister and Crawford, 1986; D'Lemos *et al.*, 1992; Davidson *et al.*, 1992, 1994; Brown, 1994a; Hutton, 1997). Also, the process of melt accumulation and its emplacement to form plutons (e.g. Paterson *et al.*, 1996; McCaffrey and Petford, 1997; Cruden, 1998; Paterson and Miller, 1998) remains contentious, and the nature of the return flow in the crust (Paterson *et al.*, 1996; Warren and Ellis, 1996; Mawer *et al.*, 1997; Weinberg, 1997; Cruden, 1998; Paterson and Miller, in press) is poorly defined.

Diapiric ascent of melt through viscous rock and ascent by flow of melt through fractures in elastic/brittle rock (dyking) represent two end-member transfer processes, but these may not be appropriate processes for the ascent of granite melt in convergent orogens. Although granites may be emplaced during orogenic collapse (Scaillet *et al.*, 1995; Brown and Dallmeyer, 1996), many granites in orogenic belts were emplaced during active contractional deformation (Brown and Solar, 1998; Paterson and Miller, in press), which implies orogen-scale (sub-) horizontal maximum principal compressive stress. Such a stress system conflicts with the general expectation in dyking that melt migrates along extensional fractures that form parallel to the maximum and normal to the minimum principal compressive stresses (Anderson, 1938, 1951). Recent work in France (Jones and Brown, 1990; D'Lemos *et al.*, 1992; Brown, 1995; Brown and Solar, 1998), Australia (Collins and Sawyer, 1996), Canada (Sawyer, 1996, 1998), New England (Solar, 1996; Brown and Solar, 1998), and the South Tibetan Himalaya (Searle *et al.*, 1997) shows that melt migration can be channeled using networks of dilatant structures and fabric anisotropies, such as foliation and lineation, which implies a significant role for deformation in deciding melt flow paths (Sawyer, 1994;

Brown and Rushmer, 1997). Porous flow in partially-molten rock and *en masse* transfer by granular flow in response to regional stress gradients are additional processes by which melt and melt plus residue may migrate in the source during contractional deformation of anisotropic crust (Sawyer, 1996, 1998; Rutter, 1997; Brown and Solar, 1998). Although the transition from porous or granular flow in the source to focussed ascent remains to be fully explained, Brown and Solar (1998) have proposed that sheet-like flow through crustal-scale shear zone systems is the ascent mechanism in convergent orogens. The change-over to channelized flow suggests rapid switches in effective permeability of the flow network caused by overpressuring, melt-enhanced embrittlement, and fracturing. Different ascent mechanisms will transfer melt through the crust at different rates (Clemens and Mawer, 1992; Clemens *et al.*, 1997; Rutter, 1997), which is likely to be an important control on the thermo-mechanical evolution of convergent orogens.

A crucial question is whether crustal anatexis synchronous with contractional deformation in convergent orogens plays a fundamental role in weakening the crust to cause faster strain rates, more rapid thickening and exhumation, and further melting in a feedback relation. Convergent orogenesis occurs at active plate margins during subduction of oceanic lithosphere and terminal continental collision. Convergence between lithospheric plates is rarely orthogonal, and the inclination of the convergence vector is a critical control on the thermo-mechanical evolution of obliquely convergent (transpressive) orogens (Robin and Cruden, 1994; Tikoff and Teyssier, 1994; Thompson *et al.*, 1997). The thermo-mechanical consequences of convergent orogenesis have been investigated using one- and two-dimensional thermal–kinematic modelling (England and Thompson, 1984; Ruppel and Hodges, 1994; Thompson and Connolly, 1995; Huerta *et al.*, 1996) and coupled thermo-mechanical models (Jamieson *et al.*, 1996, 1998; Batt and Braun, 1997). The decisive outcome of this work is that the thermal and tectonic evolution of convergent orogens are linked. Thus, during orogenesis, feedback relations are to be expected, and several examples of feedback between deformation and presence of melt have been described in the past decade (Hollister and Crawford, 1986; D'Lemos *et al.*, 1992; Neves *et al.*, 1996; Pavlis, 1996; Brown and Solar, 1998). In addition, Brown and Solar (1998) have proposed that actively deforming convergent orogens are non-equilibrium systems that generate dissipative structure by self-organization. This is expressed by the development of crustal-scale shear zone systems that control movement of granite melt through these orogens.

Melt may be arrested during ascent if the flow path intersects rheological or stress barriers, or freely slipping (sub-) horizontal fractures (Clemens and Mawer, 1992; Hogan and Gilbert, 1995), which are also likely to be important in enabling magma emplacement. Sometimes, pre-existing structures are the key to ascent and emplacement, such as the Palaeoproterozoic foliation and shear zones that provided conduits for movement of Mesoproterozoic melt into the middle crust in southwestern U.S.A. (Nyman and Karlstrom, 1997). Also, ascent may be stalled if the path intersects the water-saturated solidus, which will occur at shallower levels for low $a(H_2O)$ biotite-dehydration melting [<100 Mpa, based on the P–T diagram of Thompson (1996)] than for intermediate $a(H_2O)$ muscovite-dehydration melting [400–200 MPa, based on the P–T diagram of Thompson (1996)].

One limitation to our understanding of pluton construction is the issue of the three-dimensional shape of granites in convergent orogens. Paterson *et al.* (1996) have argued that plutons in arcs extend down through most of the crust. In contrast, McCaffrey and Petford (1997) interpret many plutons in convergent orogens to be horizontally extensive and tabular in form. If correct, this latter view suggests a fundamental change from (sub-) vertical ascent to (sub-) horizontal emplacement. This implies (sub-) vertical opening of (sub-) horizontal fractures when melt pressure exceeds the vertical load and the tensile strength of the rock. However, as Clemens *et al.* (1997) have pointed out, there is no reason to suppose that ascent and emplacement occur by the same mechanisms or at the same rates. The accumulated volume of melt is accommodated in the crust by various mechanisms, including ductile flow of wall rock, uplift of the roof and/or subsidence of the floor, dilation related to regional-scale tectonics, and stoping. Emplacement is generally the result of some combination of pluton-related and regional strains [the multiple material transfer processes of Paterson and Fowler (1993)]. Nonetheless, a strong argument has been made that these mechanisms are insufficient to create the space occupied by a pluton without downward transfer of wall rock in what Paterson *et al.* (1996) call a crustal-scale exchange process (cf. the analysis of stoping by Marsh, 1982).

This paper is one of a series that addresses the mechanisms of granite ascent and emplacement and the thermo-mechanical consequences for the crust during contractional deformation in convergent orogens (see also Brown and Solar, 1998; Solar and Brown, in press; Solar *et al.*, 1998; Pressley and Brown, in press). It is useful to characterize melt flow by reference to end-member models, such as porous flow, granular flow and channelized flow. For melt to escape the source region, however, channelized flow is necessary below the solidus. The channels do not change the permeability of the partially-molten matrix but do change the effective permeability of the flow network. Thus, to understand the process of melt extraction and transfer through the crust it is essential to understand how channelized flow is initiated and maintained—this is the focussing mechanism. To

achieve this, the spatial (porous vs channelized) and temporal (continuous vs pulsed, or slow vs fast) characteristics of melt flow paths through the anatectic zone must be identified. These data will enable us to better understand the control of melt flow by plastic deformation and to evaluate the role of melt-enhanced embrittlement. In this paper, a case study from an area in west-central Maine, which is part of the Appalachian Mountain belt, is summarized. The relationship of granite, both as leucosome in stromatic and inhomogeneous migmatites and in sheets, to regional-scale plastic deformation provides the link between flow in the source and focussed ascent through the sub-solidus crust. Concerning the important question of emplacement, in this area the three-dimensional shape of granites and their relationship to regional-scale deformation based on geological and geophysical data is deduced. Then, this information is used to develop a model for the ascent and emplacement of granite magma during contractional deformation in convergent, especially transpressive orogens.

GEOLOGY OF WEST-CENTRAL MAINE

The northern Appalachians have been divided into several tectono-stratigraphic terranes (Zen *et al*., 1986). The area of interest occurs within the Central Maine Belt (CMB) and overlaps the Ordovician rocks of the Bronson Hill Belt (BHB) to the NW (Fig. 1). To the southeast, the CMB is truncated by the Norumbega shear zone system (NSZ), along which the Neoproterozoic-to-Silurian Avalon Composite Terrane (ACT) was juxtaposed against the CMB during the Silurian–Early Devonian. In central New Hampshire and Maine, rocks within the CMB and the NSZ record dextral transpression where strain was partitioned between the dextral-transcurrent NSZ (West and Hubbard, 1997) and the dextral-reverse CMB shear zone systems (Brown and Solar, 1998).

The CMB is composed of a large volume of metasedimentary rocks (Stewart, 1989), which are interpreted to have been clastic marine sediments. Deposition of the Rangeley Stratigraphic Sequence began with coarse conglomerate of the Silurian Rangeley Formation, which was followed by deposition of finer sediment ending with the Devonian Seboomook Formation (Hatch *et al*., 1983; Moench and Pankiwskyj, 1988). The Silurian part of the sequence was derived from western sources and deposited under reducing conditions, but the Devonian part of the sequence was more likely derived from the east and deposited under oxidizing conditions. The metamorphic grade increases along strike to the southwest, from greenschist to upper amphibolite facies (Guidotti, 1989). The main penetrative deformation and metamorphism recorded within the CMB, and the associated plutonism, are the result of Devonian orogenesis (Eusden and Barreiro, 1988; Smith and Barreiro, 1990; Bradley *et al*., 1996; Solar *et al*., 1998, and references therein). Thus, deformation, metamorphism and plutonism of the sedimentary rocks in the CMB basin occurred only a short time after deposition of the sequence.

Structural framework

Deformation in west-central Maine was heterogeneous, and strain was partitioned preferentially into the rheologically weaker units. All metasedimentary rocks of the CMB exhibit high strain fabrics; they record deformation within the CMB shear zone system (Solar and Brown, in press). Mineral elongation lineation plunges, moderately-to-steeply, approximately northeast.

Detailed mapping of structures around the Tumbledown Anatectic Domain (Solar, 1996) and in the area between the Mooselookmeguntic, Redington and Phillips plutons (Brown and Solar, 1998) has enabled us to distinguish NE-trending, steeply SE-dipping zones of pervasively parallel structural elements that anastomose around lenses in which structural elements are non-parallel (Fig. 1). In rocks that remained below the contemporary solidus, these contrasting structural domains are distinguished based on fabric style. $S \geq L$ fabrics occur in the zones of parallel strike-of-foliation form lines to suggest general flattening-to-plane strain. In the intervening lenses, mineral elongation lineation is pervasively developed but foliation is weak or absent, suggesting $L \gg S$ fabrics and constrictional strain. Although planar structural elements in these lenses are generally non-parallel at map scale, reflected in the trend of strike-of-foliation form lines in Fig. 1, mineral elongation lineations and fold hinge lines are sub-parallel to each other where they occur together in outcrop. We interpret these structural characteristics to reflect partitioning and localization of strain and we interpret the steeply SE-dipping zones of pervasively parallel structural elements to record higher strain (higher strain zones, HSZs) that anastomose around lenses in which structural elements are non-parallel and reflect lower strain (lower strain zones, LSZs). This pattern can be seen from the regional scale to the thin section scale.

A similar range of compositions is represented by rocks in both HSZs and LSZs but in different proportions, with a higher ratio of pelite to psammite in units that have localized the higher strain; rocks in both HSZs and LSZs record similar microstructures (Solar and Brown, in press). The structural boundaries shown on Fig. 1 are placed at the sharp change between zones of apparent flattening-to-plane strain (HSZs) and zones of apparent constrictional strain (LSZs). These observations are consistent with results obtained from analytical and analog modeling (Cruden and Robin, 1997; Robin and Cruden, 1997), which show that under different conditions of viscosity

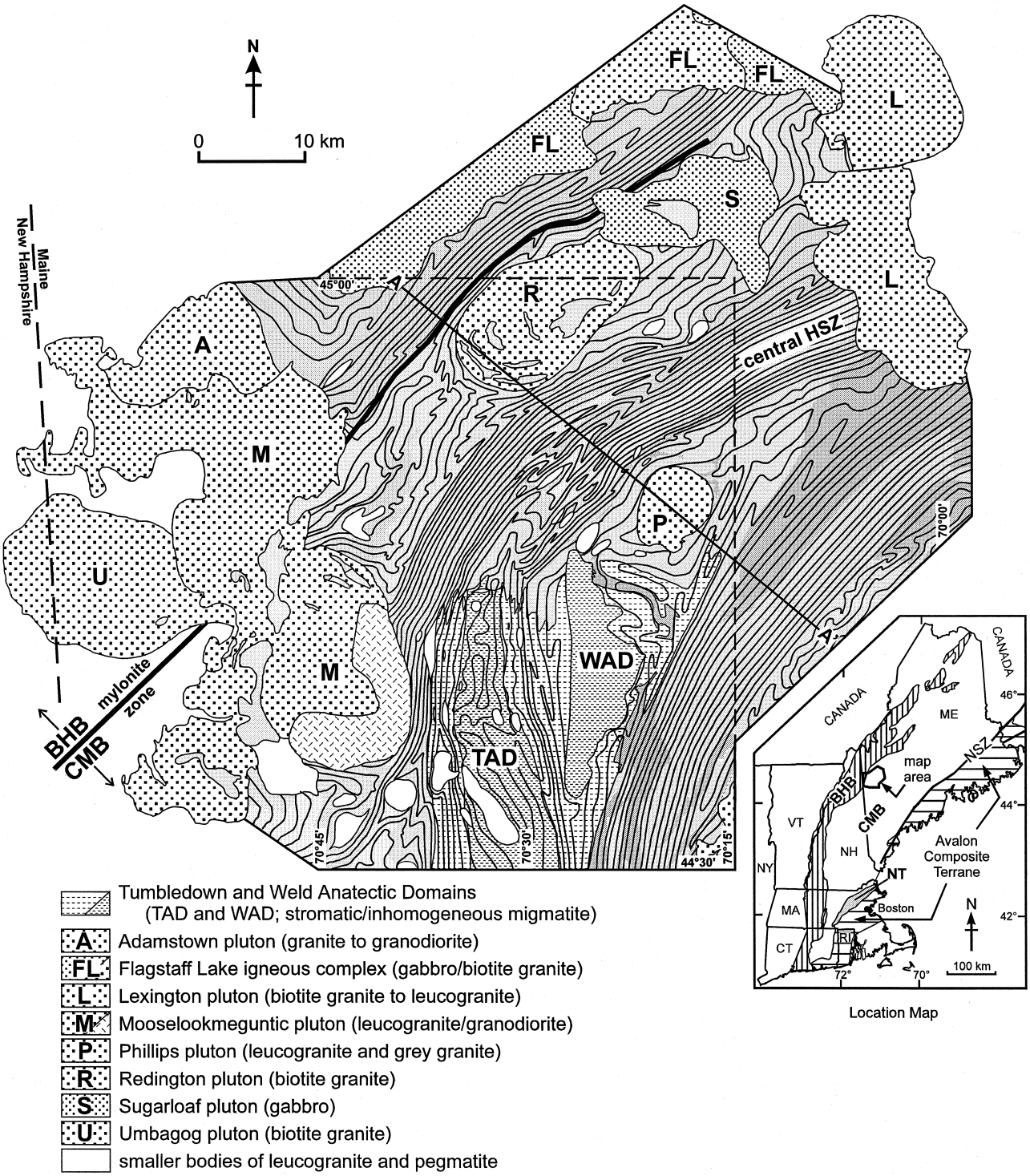

Fig. 1. Simplified geological and structural form line map of a portion of west-central Maine and adjacent New Hampshire, U.S.A. The geology inside the area south and west of the dashed lines (44°30′ to 45°00′ N; 70°15° W to the Mooselookmeguntic pluton) is based on a combination of detailed new mapping (Solar, 1996; Brown and Solar, 1998) and extensive field checking of data represented on the maps of Moench (1971), Moench and Hildreth (1976) and Pankiwskyj (1978). Outside of this area, the geology is based on the map of Moench *et al.* (1995), corroborated by limited field checking of structures and lithologic contacts, and extrapolation of structures to the northeast from the area of our more detailed work as far as the Lexington pluton. Solid lines are strike-of-foliation form lines (in metasedimentary rocks). Foliation dips generally southeast and closeness of form lines denotes steepness of dip (closely-spaced—steeply-dipping; widely-spaced—moderately-dipping). Field data (Solar, 1996; Brown and Solar, 1998) supported by microstructural observations (Solar and Brown, in press) confirm that areas of pervasively-parallel and closely-spaced strike-of-foliation form lines correlate with higher strain (HSZs, as discussed in the text) and areas of variable trend with widely-spaced form lines correlate with areas of lower strain (LSZs). The Rangeley Stratigraphic Sequence is represented by various grey ornaments. BHB is the Bronson Hill Belt and CMB is the Central Maine Belt; A–A′ line of section in Fig. 5. On the location map, ME is Maine, NH is New Hampshire, VT is Vermont, NY is New York, MA is Massachusetts, CT is Connecticut and RI is Rhode Island; NSZ is the Norumbega Shear Zone System and NT is the Nashoba Terrane.

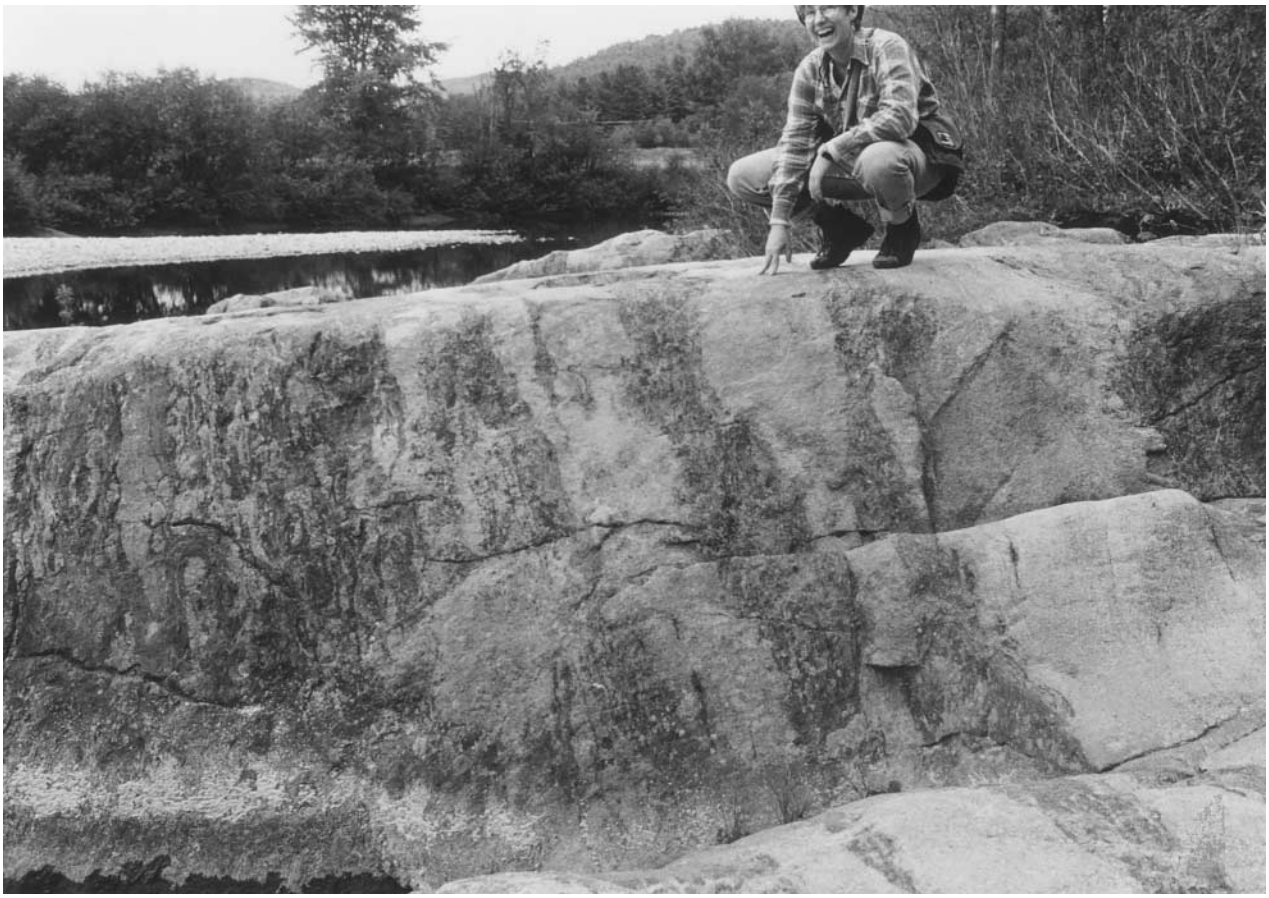

Fig. 2. Steeply E-dipping granite sheets in stromatic migmatite within the central high strain zone, west of the Tumbledown Anatectic Domain, Central Maine Belt, west-central Maine (steeply E-dipping fabric, view to north).

contrast and convergence angle, HSZs can record general-to-strongly flattening strains while simultaneously LSZs record plane strain with well-developed lineation.

Dextral-reverse oblique shear is shown by asymmetric boudinage in outcrop, and corroborated by asymmetric porphyroblast–matrix–tail relations in thin sections cut parallel to mineral elongation lineation and normal to foliation (Solar and Brown, in press). Metamorphism occurred at middle crustal depths (Guidotti, 1989; Guidotti and Holdaway, 1993); porphyroblast inclusion trail–matrix foliation relationships in appropriately oriented thin sections show that metamorphic crystallization and plastic deformation were regionally synchronous (Solar and Brown, in press). Monazite separated from samples of pelitic schist at staurolite grade from the central HSZ yields metamorphic ages of 405–399 $\pm$ 2 Ma (Smith and Barreiro, 1990), which we interpret to be the age of plastic deformation. In contrast, monazite separated from samples of pelitic schist spatially associated with the granodiorite phase of the Mooselookmeguntic pluton around its southeast side, yields ages of 374–363 $\pm$ 2 Ma, interpreted to be the result of recrystallization during contact metamorphism, consistent with a crystallization age for the granodiorite phase of 363 $\pm$ 2 Ma (Smith and Barreiro, 1990), which probably dates emplacement of this unit.

Migmatites and granites

Displacement accommodated by the CMB shear zone system was dextral-reverse, so that blocks on the southeast side were obliquely thrust inboard to the northwest and along strike to the southwest (Brown and Solar, 1998). Thus, the block to the southeast of the central HSZ exposes a deeper structural level than the block to the northwest, from the central HSZ to the mylonite zone, and the BHB farther northwest represents a still higher structural level. Within any block, the southwest side of the exposed surface is the deeper level, with shallower levels exposed to the northeast along the trend of the mineral elongation lineation. Thus, the deepest structural levels within the area of Fig. 1 are represented by the Weld Anatectic Domain (WAD) and the Tumbledown Anatectic Domain (TAD).

Migmatitic rocks are spatially restricted to the WAD and TAD (Fig. 1), which have sharp contacts with non-migmatitic rocks. Within these domains, we have divided the migmatites into stromatic and inhomogeneous types (Solar, 1996; Brown and Solar, 1998). The distribution of these different migmatite types correlates with structures (Fig. 1). Stromatic migmatites (Figs 2 & 3) occur in HSZs, while inhomogeneous migmatites (Fig. 4) occur within elongate

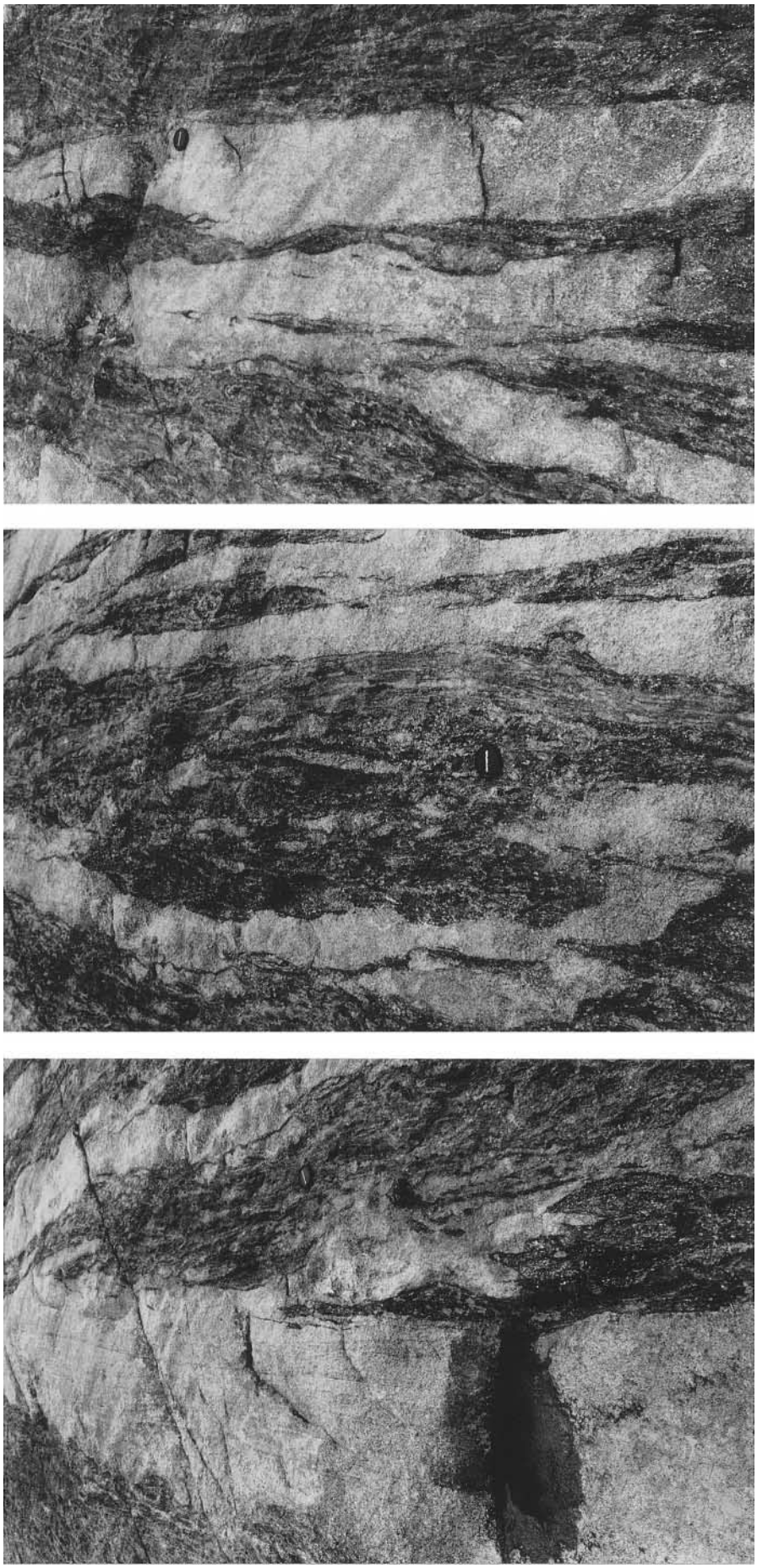

Fig. 3—*Caption opposite.*

areas at map scale that correspond to LSZs, and their elliptical map outlines reflect oblique sections through these domains of constrictional strain. The map outlines are asymmetric, consistent with dextral kinematics and the geometry of structures at a regional-scale. As the CMB shear zone system passes through west-central Maine (Fig. 1), attitudes of structural elements in the central HSZ change in strike (relict bedding and foliation) and in trend (linear structures) from northeast to north and from northeast to south across the area (Brown and Solar, 1998), and revert to northeast farther southwest (Moench *et al*., 1995); concurrently, mineral elongation lineation and fold hinge lines vary from moderately-plunging to steeply-plunging and back to moderately-plunging. This geometry and the map patterns suggest that this part of the CMB shear zone system in west-central Maine forms a transpressive restraining bend, within a regional-scale dextral-reverse structure. The inhomogeneous migmatites are concentrated within the asymmetric LSZs in the region of the bend.

The approximate coincidence of foliation and migmatite leucosomes in HSZs and the occurrence of concordant to weakly-discordant irregular granite sheets (Figs 2 & 3) suggest that melt migrated along the foliation or in sheet-like bodies parallel to or at a low angle to the foliation (Brown and Solar, 1998). In detail, on both shallowly-oriented and steeply-oriented surfaces, these granite sheets exhibit pinch and swell structure (Figs 2 & 3), although no solid-state deformation is recorded by the granite. This suggests that accumulation of plastic strain outlasted upward movement of the granite, but that final crystallization of the granite outlasted deformation. Magmatic flow structures in granite, such as multiple sheeting, asymmetric biotite-rich schlieren and trails of residual biotite crystals show that granite in sheets is exotic to the outcrop in which it occurs. Although the migmatite leucosomes are likely to be locally-derived, they may represent melt frozen during syntectonic migration through the stromatic structure, rather than stagnant melt crystallized *in situ* (Brown *et al*., 1995; Brown and Brown, 1997). The stromatic leucosomes have higher aspect ratios in sections approximately parallel to lineation compared to sections at a high angle to lineation, consistent with flattening-to-plane strains. Inhomogeneous migmatites exhibit flow structures similar to those seen in granite sheets, and show leucosome concentrations at tails of enclaves (Fig. 4) that demonstrate melt segregation during flow (Sawyer, 1996).

Based on these observations, we interpret the CMB shear zone system to form a percolation network that focused melt flow through the crust (Brown and Solar, 1998). We do not agree with the view that migmatites represent failed systems with little relevance to crustal-scale melt flow. Instead, we speculate that lower crustal migmatites at both amphibolite and granulite facies grade of metamorphism preserve evidence of the mesoscopic melt flow paths in the source regions of granite plutons. As in any detective method, we are working with incomplete and imperfect evidence. Nonetheless, prosecuting an understanding of melt flow in migmatites will provide more realistic constraints on models of granite extraction from the anatectic zone.

A higher volume percent leucosome is preserved in inhomogeneous migmatites than in stromatic migmatites, which suggests that more melt may have been generated and retained in the inhomogeneous migmatites, or that melt infiltrated the LSZs. All gradations exist between dark inhomogeneous migmatites with a residual aspect and schlieric granite, which indicates melt migration through the partially-molten system. Although the stromatic migmatites preserve a lower volume percent leucosome, which may imply that less melt was generated and retained in these rocks, the residual nature of some stromatic migmatites, which is implied by mineral modes of melanosomes, suggests that melt has been driven out of these rocks as well. Melt loss from structurally deeper levels is represented by granite sheets in the stromatic migmatites and schlieric granites in the inhomogeneous migmatites. We are in the process of gathering geochemical data to evaluate melt loss from inhomogeneous and stromatic migmatites.

Magmatic zircon and monazite separated from samples of three syn-kinematic leucogranite sheets lodged within the central HSZ yield ages of 408.2 ± 2.5 Ma, 407.9 ± 1.9 Ma and 404.3 ± 1.9 Ma, from south to north along the zone, interpreted to date crystallization closely (Solar *et al*., 1998). There are three principal Early Devonian granite plutons: the Redington pluton (407.6 ± 4.7 Ma, Solar *et al*., 1998); the Phillips pluton (403.8 ± 1.3 Ma, Pressley and Brown, in press; see also Solar *et al*., 1998); and, the Lexington pluton (404.2 ± 1.8 Ma, Solar *et al*., 1998). The *ca* 404 Ma age for the Lexington pluton is consistent with a Rb–Sr whole-rock age of 399 ± 6 Ma (Gaudette and Boone, 1985; see also Dickerson and Holdaway, 1989). Given the proximity of these plutons to migmatites exposed in the TAD and WAD (Fig. 1), and the

Fig. 3. Shallowly W-inclined surface that cuts steeply E-dipping granite sheets in stromatic migmatite (see Fig. 2) within the central high strain zone, west of the Tumbledown Anatectic Domain, Central Maine Belt, west-central Maine (steeply E-dipping fabric, view to south; top photograph east part of outcrop, centre photograph centre part of outcrop, bottom photograph west part of outcrop). The granite sheets vary from concordant to weakly discordant with respect to migmatitic foliation, which implies control by the fabric anisotropy on sheet geometry, and may show pinch-and-swell structure. Magmatic foliation, defined by multiple sheeting and biotite schlieren, most prominently displayed in the largest sheet in the top photograph, is generally (sub-) parallel to sheet margins.

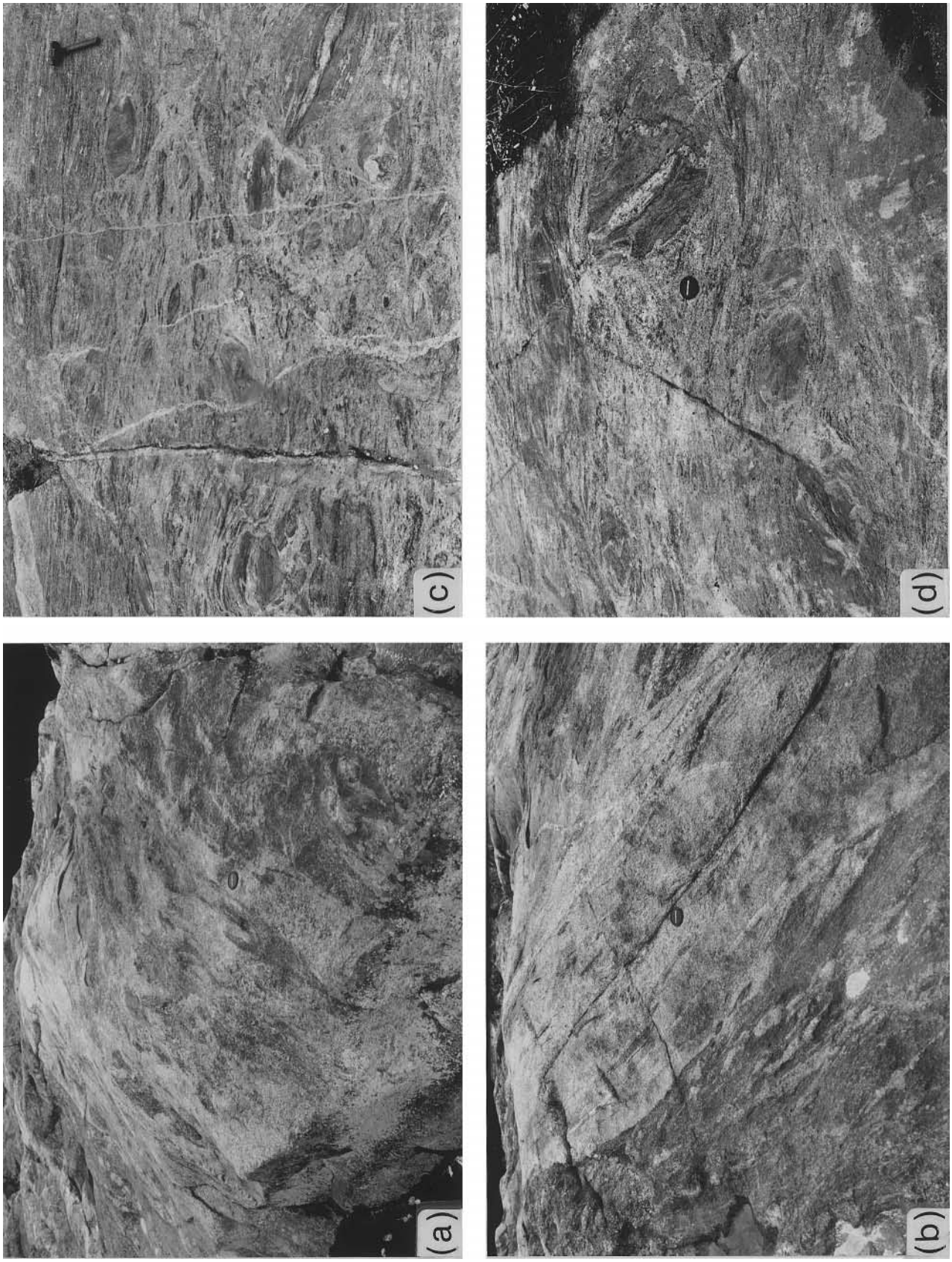

Fig. 4—*Caption opposite.*

down-plunge projection of the WAD beneath the Phillips pluton, it is to be expected that most of the melt that accumulated to form these plutons was derived from a metasedimentary source similar to the CMB rocks at outcrop. This has been confirmed for the Phillips pluton using REE geochemistry and the isotopic composition of Nd (Pressley and Brown, in press). In the west, the Mooselookmeguntic pluton and associated bodies (Fig. 1) underlie >1000 km^2 of the area and represent the largest Devonian pluton in west-central Maine. This pluton is the youngest of the four granites, two of the units within it having yielded crystallization ages of 388.9 ± 1.6 Ma and 370.3 ± 1.1 Ma, respectively (Solar *et al.*, 1998). The Mooselookmeguntic pluton extends across the boundary between the BHB and CMB, and consequently some granite magma within the pluton might have been derived from the BHB, although this remains to be tested using geochemical data.

INFERENCES ABOUT EMPLACEMENT FROM PLUTON GEOMETRY

The three-dimensional form of plutons can be deduced by combining geological information with models based on geophysical data, in particular gravity studies. In this paper a regional view is taken. To derive pluton geometries, the data used are: (1) new mapping and recently-collected structural data (Solar, 1996; Brown and Solar, 1998); (2) extant mapping (e.g. Moench *et al.*, 1995, and work referenced therein); (3) thermal aureole width and depth of pluton emplacement [as represented by metamorphic mineral assemblages; summarized in Guidotti and Holdaway (1993), and work referenced therein]; (4) cross-sections of plutons modelled in a regional gravity study of the western part of the area (Carnese, 1981); and (5) a crustal model constructed after a detailed integrated geophysical study in the eastern part of the area (Stewart, 1989; Unger *et al.*, 1989). It is appreciated that the pluton geometries derived here are speculative because of restrictions imposed by the amount of outcrop and the limited size of the gravity dataset, and the intrinsic limitations in modelling of residual gravity anomalies. In addition, downward thicknesses estimated from gravity data represent minima since the proportion of each pluton removed by erosion cannot be deduced, except where part of the roof contact is preserved or the metamorphic imprint beneath the floor of the removed granite remains.

The plutons are described in three groups (Figs 1 & 5): within the block to the southeast of the central HSZ (the Phillips pluton and the associated WAD); those in the block to northwest of the central HSZ (Redington and Lexington plutons); and the younger Mooselookmeguntic pluton and associated bodies that cut across the mylonite zone separating the BHB and the CMB. Given the implication of the dextral-reverse kinematics that successively shallower structural levels are exposed to the northwest and the crystallization ages of the four plutons, this sequence is a progression from contemporaneous deeper to shallower levels across the central HSZ, and to regionally cooler crust at the time of emplacement of the Mooselookmeguntic pluton (Guidotti, 1993; Guidotti and Holdaway, 1993).

The Phillips pluton

The Phillips pluton is composed of dominantly medium–coarse-grained two-mica leucogranite and subordinate fine–medium-grained granodiorite (Pressley and Brown, in press). It is subcircular in map view, ~8 km in diameter, and is in the LSZ to the southeast of the central HSZ (Figs 1 & 5). Magmatic fabrics (planar biotite-rich schlieren, and modal and grain-size layering) occur locally in the leucogranite and are oriented conformably with the NE-striking foliation in the surrounding metasedimentary units. Where observed, local contacts between granite and metasedimentary rocks are concordant with respect to regional structure; pluton contacts are steeply SE-dipping on the northwest and southeast sides of the pluton, and apparently NE-dipping on the northeast side. At its margins, the Phillips pluton records no solid-state deformation of the kind commonly attributed to ballooning, and there is no discrete metamorphic aureole separable from the regional metamorphism. Emplacement is interpreted to have occurred during active deformation synchronous with the peak of regional metamorphism. The pressure of metamorphism around the Phillips pluton was ~400 MPa [based on the production of sillimanite rather than andalusite by the reaction muscovite + staurolite + chlorite +

Fig. 4. (a) and (b) Foliated schlieric granite in steeply E-dipping sheet that cuts stromatic migmatite within the central high strain zone, west of the Tumbledown Anatectic Domain, Central Maine Belt, west-central Maine (same outcrop as Figs 2 and 3, west extremity of outcrop close to water level in stream). The photograph in (a) is a view to the south, and the photograph in (b) is a view of the shallowly W-inclined surface of the outcrop to show the weak discordance of the sheet margin with the foliation in the stromatic migmatite. (c) and (d) Foliated inhomogeneous migmatite at the transition between stromatic and inhomogeneous migmatite domains at the eastern margin of the central high strain zone (north to left), Tumbledown Anatectic Domain, Central Maine Belt, west-central Maine. Notice the higher volume percent leucosome and schlieric structure (absence of regular compositional layering and presence of residual biotite aggregated in clumps) of the inhomogeneous migmatite in comparison with the stromatic migmatite shown in Fig. 3. The schlieren define a flow foliation that surrounds calc-silicate enclaves [below and to left of lens cap in (d)] included within the migmatite.

quartz → sillimanite + biotite + H_2O (Guidotti, 1974; Guidotti *et al.*, 1991), using the petrogenetic grid of Pattison and Tracy (1991); and, using the muscovite–almandine–biotite–sillimanite geobarometer (Holdaway and Mukhopadhyay, 1996; Holdaway, pers. comm.).

Our structural interpretation of the Phillips pluton is that it has a steeply SE-dipping sheeted internal structure with a hemi-ellipsoidal form in three-dimensions, the long axis of which plunges parallel to the moderately NE-plunging mineral elongation lineation in the country rocks. A funnel-shaped body has been suggested in a three-dimensional geological model constructed from combined geophysical and geological data (Unger *et al.*, 1989). The −10 mgal residual gravity contour (Carnese, 1981) is taken to outline the melt ascent conduit or 'root zone' of the pluton (Fig. 5). We infer that melt ponded and crystallized within the LSZ. Pinch and swell structure of leucogranite sheets discordant to foliation in the thermal aureole suggests that waning ductile deformation was not finished at the time of emplacement of the Phillips pluton (Pressley and Brown, in press). We infer from this that the exposed level represents the part of the pluton below the level of the contemporary brittle–plastic transition. It is plausible that the Phillips pluton extended laterally at shallower levels as a tabular pluton removed by erosion, but there is no information to constrain such speculation (Guidotti and Holdaway, 1993).

The WAD is poorly exposed; although mapped by Moench and Pankiwskyj (1988) as part of the Phillips pluton, Brown and Solar (1998; see also Pressley and Brown, in press) interpret it to be inhomogeneous migmatite with lenses of schlieric granite. Given the moderate-to-steeply NE-plunging mineral elongation lineation in the CMB rocks (Brown and Solar, 1998), it is implicit that rocks similar to these inhomogeneous migmatites with lenses of schlieric granite underlie the Phillips pluton (Fig. 1). An important conclusion of work on the Phillips pluton is confirmation from the isotopic composition of Nd that it is composed of multiple batches of melt (Pressley and Brown, in press), as implied by the sheeted structure observed at outcrop. A second significant conclusion from this study (Pressley and Brown, in press) is that the leucogranite that comprises most of the pluton was derived from a source with similar isotopic composition to the surrounding CMB rocks, although the minor granodiorite has an isotopic composition compatible with derivation from Avalon-like crust inferred to underlie the CMB rocks (Stewart *et al.*, 1992).

The Redington pluton

The Redington pluton is predominantly a porphyritic biotite granite. It has an oval map shape elongate NE–SW, with axial dimensions of $\sim 20 \times 10$ km, and is in the LSZ to the northwest of the central HSZ (Figs 1 & 5). The pluton has irregularly NE-dipping contacts with country rocks in the northeast and inward-dipping contact in the southwest (Moench and Zartman, 1976), where it is inferred to be in contact with country rocks along a NE-dipping surface that represents the base of the pluton. In the southwest, aligned K-feldspar phenocrysts define a moderately NE-dipping magmatic foliation inside the pluton, subparallel to km-scale screens of weakly strained hornfelsic wall rock. The thermal aureole associated with the pluton is narrow, generally < 1 km wide. Based on the succession of metamorphic mineral assemblages towards the contact in muscovite–quartz–ilmenite–graphite-bearing pelites [andalusite + cordierite + biotite succeeded by sillimanite + K-feldspar + cordierite + biotite and 'very little staurolite or garnet'; from Guidotti and Holdaway (1993)], we estimate metamorphic P of not less than ~300 MPa using the petrogenetic grid of Pattison and Tracy (1991). Foliation trajectories in the country rocks on the southwest side are interpreted to reflect interaction between pluton emplacement and regional foliation development, and suggest intrusion during active plastic deformation, with melt flow likely to the southwest during emplacement (Cruden and Launeau, 1994).

A model interpretation of gravity data suggests a horizontal wedge as much as 2.5–3 km thick at the northeast end thinning to the southwest (Carnese, 1981). The −10 mgal residual gravity contour (Carnese, 1981) is taken to outline the melt ascent conduit or 'root zone' of the pluton (Fig. 5); it is offset to the northeast, which is consistent with the root zone extending down the lineation, although the strong positive gravity anomaly associated with the Flagstaff Lake igneous complex may displace the anomaly to the southeast. From this it is inferred that melt ponded in the LSZ. Space for emplacement was created by a combination of stoping screens of wall rock and wall-rock deformation at the leading edge during intrusion to the southwest (Fig. 1), possibly in association with some lifting of the roof and/or sinking of the pluton floor, the latter suggested by the slope of the pluton floor down-to-the-NE (Fig. 5). The relative contribution of each of these potential space-creation mechanisms in accommodating the inferred southwest flow of the inflating magma wedge has not been estimated. Based on the style of granite intrusion, we suggest that the Redington pluton was emplaced around the level of the contemporary brittle–plastic transition.

The Lexington pluton

The Lexington pluton, which is the thickest pluton in the area, comprises a northern and central-southern lobe (Figs 1 & 5). The northern lobe, which has axial dimensions of $\sim 15 \times 12$ km, is composed of biotite granite; it exhibits dextral offset with respect to the

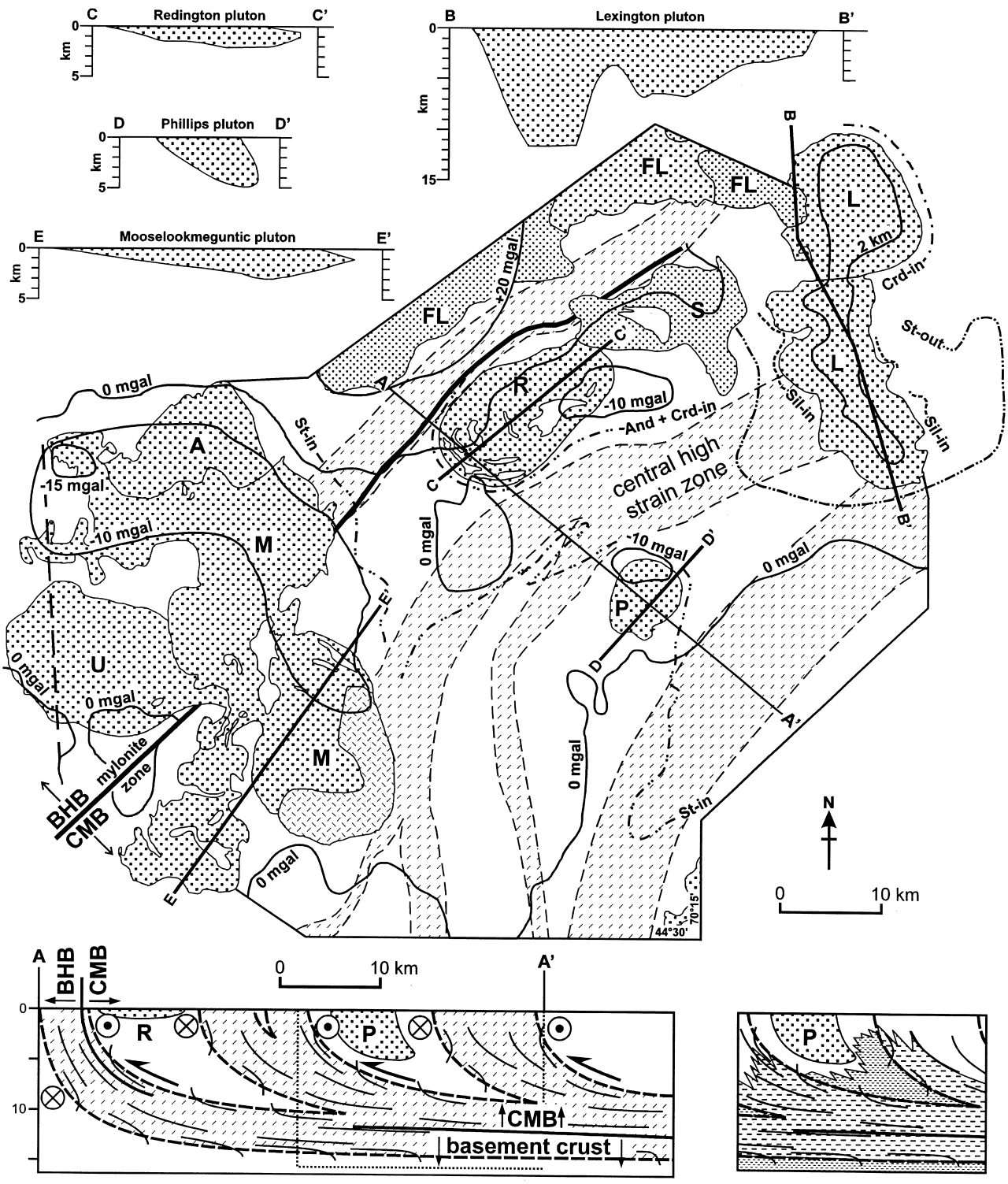

Fig. 5. Map to show the relationship between granite plutons and the shear zone system. Contours of residual gravity are taken from Carnese (1981). The 2 km contour of depth to the contact beneath the Lexington pluton is taken from Unger *et al.* (1989); maximum depth to the floor varies along the pluton from ~12 km in the northern lobe to 6–3 km from north-northwest to south-southeast along the central-southern lobe. HSZs are indicated by the inclined dashes, and LSZs are unornamented; plutons are indicated in various dotted ornaments, given in Fig. 1. An indication of the extent of the metamorphic aureole surrounding each pluton is given by an appropriate isograd (see text for details). A–A′ is the line of the true-scale section shown beneath the map at left. Solid lines represent the intersection of foliation planes with the plane of the section. Part of the section is redrawn to the right to show migmatite type (ornaments the same as in Fig. 1) predicted to occur at depth beneath the Phillips pluton as a consequence of the moderate-to-steeply NE-plunging regionally-developed mineral elongation lineation.

central-southern lobe. The central-southern lobe, which has axial dimensions of $\sim 20 \times 10$ km, is composed of porphyritic and two-mica granites; Williamson and Seaman (1996) interpret magma mingling textures at lower elevations to represent interaction between infusions of mafic magma and the partially-crystallized granite into which it was emplaced. The northern lobe is in the LSZ to the northwest of the central HSZ; a thermal aureole was produced up to ~1.5 km wide (Dickerson and Holdaway, 1989). Based on the succession of metamorphic mineral assemblages towards the contact in muscovite–quartz–ilmenite–graphite-bearing pelites [cordierite + biotite + chlorite, andalusite + cordierite + biotite, and sillimanite + K-feldspar + cordierite + biotite; from Dickerson and Holdaway (1989)], we estimate metamorphic P of ~300 MPa using the petrogenetic grid of Pattison and Tracy (1991).

The central-southern lobe cuts across the strike of the central HSZ (Fig. 1). Around the central-southern lobe, the thermal aureole expands from ~1.5 km at the central part to ~8 km on both the WSW and ENE of the southern part, before narrowing to ~1.5 km at the south end of the pluton (Dickerson and Holdaway, 1989). Based on the succession of metamorphic mineral assemblages towards the contact in muscovite–quartz–ilmenite–graphite-bearing pelites [andalusite + staurolite + biotite $\pm$ garnet, andalusite + biotite + garnet, and sillimanite + biotite + garnet; from Dickerson and Holdaway (1989)], we estimate metamorphic P of 300–350 MPa using the petrogenetic grid of Pattison and Tracy (1991). The pluton is characterized by a large negative gravity anomaly (Unger *et al.*, 1989). Since there is no geophysical evidence in support of the pluton extending below the wide thermal aureole in the southern part, Stewart (1989) postulated that originally the pluton was more extensive in a WSW–ENE direction above the thermal aureole. If correct, this implies a shallow, inward-dipping pluton floor to the WSW and ENE sides of the exposed central-southern lobe, which extended outward and upward to an unknown level in the crust above the exposed level, which raises the minimum width of this lobe to at least 35 km.

Modelling by Unger *et al.* (1989) suggests the northern lobe is ~12 km thick, with steep inward-dipping contacts, in comparison with the central-southern lobe, which thins from ~6 to ~3 km across the strike of the central HSZ (Fig. 5). Thus, the Lexington pluton has hybrid geometry. We infer that the northern lobe was formed by crystallization of melt that ponded in the LSZ, whereas the cross-cutting central-southern lobe represents melt possibly emplaced in a (sub-) horizontal fracture. Seismic reflection data show that the floor of the pluton is not sharp against the wall rock; there is a zone of $\approx$2 km thick where energy is weakly reflected, which is inconsistent with expectations for homogeneous granite (Stewart, 1989). One plausible interpretation of this zone is that it comprises sheets of granite interleaved with wall rock, possibly in similar fashion to the southwest part of the Redington pluton.

We postulate that fracture propagation for emplacement of the central-southern lobe of the Lexington pluton was across structure to the SSE along the length of the pluton and in the direction of thinning. We suggest further that fracture propagation from the northern lobe along the LSZ to the WSW may have been inhibited by the older Sugarloaf pluton (K–Ar biotite age of *ca* 406 Ma, recalculated from Zartman *et al.*, 1970), which has been overprinted by the contact metamorphic aureole of the Lexington pluton. To the northwest is the Flagstaff Lake igneous complex, which is within the older Bronson Hill Belt. We speculate that these rheologically strong isotropic plutonic complexes forced fracture propagation to the SSE across the anisotropy as a result of the presence of the rheologically weaker CMB rocks on that side of the ascent conduit.

Space creation to allow inflation could possibly have occurred by sinking of the pluton floor and/or lifting of the roof. However, the combination of 'flats' and 'ramps' along the floor (Fig. 5), in which the 'ramps' correspond to HSZs, suggests that reverse displacement along the CMB shear zone system was occurring during emplacement. We interpret the level of emplacement, as exposed, to correspond approximately to the contemporary brittle–plastic transition, but speculate that if the southern part was more laterally extensive within 1 km above this level, it may have been emplaced in a more extensive (sub-) horizontal fracture that propagated laterally in an arc from the WSW to the ENE similarly to that postulated below for the Mooselookmeguntic pluton.

The Mooselookmeguntic pluton

The Mooselookmeguntic pluton is the largest of the four plutons (Figs 1 & 5); it is composed of predominantly two-mica granite, which, locally, may contain disoriented blocks of granodiorite/tonalite. On the east side, the contact with CMB metasedimentary rocks is outward-dipping, shallow in the north and moderate in the south; on the south side, the contact dips shallowly to the south; in the northwest, the contact dips to the northwest; and, in the west, the contact dips to the west (Moench and Zartman, 1976). In the western part of the pluton, an irregular contact separates underlying granite from overlying CMB metasedimentary rocks at higher elevations. On the east side, there is a thermal aureole generally of 2–5 km width (Moench and Zartman, 1976). The pressure of metamorphism around the Mooselookmeguntic pluton was ~400 MPa [based on the production of sillimanite rather than andalusite by the reaction muscovite + staurolite + chlorite + quartz $\rightarrow$ sillimanite + biotite + H_2O (Guidotti, 1974; Guidotti *et al.*, 1991), using the

petrogenetic grid of Pattison and Tracy (1991); and, using the muscovite–almandine–biotite–sillimanite geobarometer (Holdaway and Mukhopadhyay, 1996; Holdaway, pers. comm.)]. On the southeast side, the two-mica granite is surrounded by a younger granodiorite that is discordant with the central HSZ (Fig. 1); it is interpreted as a thin (sub-) horizontal sheet.

Based on modelling of gravity data (Carnese, 1981), the two-mica granite of the main pluton has a tabular form as much as 4 km thick on the northern and eastern sides, wedging out in country rock to the north, east and south, and thinning to the southwest above a shallow NE-dipping floor. The 'root zone' is outlined by the −15 mgal contour of residual gravity (Carnese, 1981) in the northwest of the pluton, and the deeper part of the pluton in the north and east, outlined by the −10 mgal contour of residual gravity (Carnese, 1981), crosses structures to the SSE, in a similar fashion to the Lexington pluton (Fig. 5). We infer that melt intruded into a propagating fracture with melt flow towards the southwest. Although stoping is implied by locally-derived blocks along unit margins, we speculate that most of the space creation to allow inflation occurred by lifting of the roof and/or sinking of the pluton floor, the latter suggested by the slope of the pluton floor down to the north and east. The discordant nature of pluton margins to terrane boundaries and to regional foliation is consistent with this being the youngest pluton in the area; we suggest that the Mooselookmeguntic pluton was emplaced close to, but above, the contemporary brittle–plastic transition.

Summary

The Phillips pluton was formed in an LSZ and the granite simply solidified where it had accumulated as ascent became inhibited. If this pluton does represent an ascent conduit for a more extensive horizontal tabular granite removed by erosion, then we presume that ascent became inhibited at the present level because the rate of pluton inflation had become negligible at a shallower level due to solidification of the melt. The Redington pluton is the oldest of the four granites; it represents melt that ponded in an LSZ, and we speculate that ascent became stalled because the path intersected the solidus. We suggest that the local balance of forces enabled lateral flow to the southwest along the LSZ and the formation of a wedge-like pluton during active plastic deformation and foliation formation in the CMB rocks. The Lexington pluton is interpreted to represent a hybrid emplacement mechanism in which one part has maintained a deep root, while in the other part melt was intruded across-strike in a (sub-) horizontal fracture. Finally, the Mooselookmeguntic pluton is the youngest of the four granites; it appears that melt was emplaced in a (sub-) horizontal fracture that propagated from the north to the south-southeast and to the southwest. Based on emplacement style, it is inferred that the brittle–plastic transition occurred at ∼10 km depth contemporaneous with emplacement of the Redington, Lexington and Phillips plutons, but had subsided to ∼13 km depth by the time of emplacement at the Mooselookmeguntic pluton.

A model for granite ascent and emplacement during active contractional deformation in convergent, especially transpressive orogens is developed using information from the analysis of granites in west-central Maine. To do this, it is necessary to consider the influence of deformation on melt flow and the driving forces for granite ascent. These issues are addressed in the next two sections.

DEFORMATION AND FLUID FLOW, WITH PARTICULAR REFERENCE TO CRUSTAL MELTS

Fluid flow in the crust

Modelling of processes in the upper crust has been directed towards understanding the development of fluid overpressure under hydrostatic conditions (Walder and Nur, 1984; Gavrilenko and Geugen, 1993). At greater depth in the crust, however, a large quantity of aqueous fluid is released by devolatilization reactions during prograde metamorphism (Fyfe *et al.*, 1978; Connolly, 1997a; Wong *et al.*, 1997), which generates fluid overpressures in the metamorphic realm. Thus, in the lower crust, the fluid-pressure gradient is likely to be close to lithostatic (Fyfe *et al.*, 1978), although a strictly lithostatic pressure distribution will be the exception rather than the rule (Turcotte and Schubert, 1982), and fluid pressure oscillates about the lithostatic because of compaction processes (Connolly, 1997a). The fluid flows down the hydraulic gradient, generally upwards from depth to the Earth's surface, driven by buoyancy forces, fluid pressure and tectonic overpressure, at rates controlled by the relationship between porosity and permeability, and the viscosities of the matrix and the fluid. The processes involved are poorly understood (Ferry, 1994a; Rumble, 1994).

Experimentally determined values for the equilibrium fluid–solid dihedral angles in geological systems predict a connected grain-edge porosity for aqueous fluids (see review by Holness, 1997 and references therein). Deformation influences fluid flow because it can enhance or restrict permeability (e.g. by fracturing or opening grain boundaries, or by closing such features during shear-enhanced compaction), and cause changes to the porosity or pore geometry as a result of plastic strain (Etheridge *et al.*, 1984; Knipe and McCaig, 1994), particularly during metamorphic devolatilization or melting, leading to the idea of dynamic permeability (Stephenson *et al.*, 1994; Holness, 1997).

Also, dynamic wetting of grain boundaries may occur during active deformation (e.g. Tullis *et al.*, 1996).

Pervasive migration of aqueous fluid occurs by porous flow, and it is common for flow to occur preferentially along shear zones or in high porosity channels (O'Hara, 1994; Connolly, 1997a; McCaig, 1997). As Connolly (1997a) has pointed out, the rocks that overlie a metamorphic devolatilization front cause the fluid pressure gradient in the reacting crust to diverge from lithostatic, ultimately leading to dilational deformation in which the reacting crust undergoes compaction and a wave of anomalous fluid pressure and porosity is driven upward. This pulsed flow can vary from highly episodic to quasi-steady-state. If the rate of aqueous fluid production exceeds the rate of migration by porous flow, transient hydrofracturing may occur (Nakashima, 1995; Brantley *et al.*, 1997). The increasing level of supported differential stress with decreasing depth in the crust below the brittle–plastic transition enhances the likelihood of hydrofracture.

In principle, migration of granite melt through the anatectic zone in the crust is comparable with metamorphic fluid flow, and the evolution of melt pressure during crustal anatexis is analogous to the evolution of fluid pressure during prograde regional metamorphism. Above the solidus, quartz-bearing crustal rocks have pore connectivity of the melt phase (Laporte and Watson, 1995; Holness, 1997); in partially-molten rocks connectivity occurs at low melt fraction and the permeability threshold is low (Laporte *et al.*, 1997). Differences between melt flow and metamorphic fluid flow relate to the intrinsic properties of the melt, which is more viscous with a higher density, and to the question of flow outside the anatectic zone.

As shown by McKenzie (1984, 1985) viscous porous media will initially compact over a characteristic length-scale, with a characteristic time-scale for fluid loss from the scale of the compaction length or from the whole compacting region. Theoretical and numerical modelling of melt flow through a deformable matrix show that the porosity structure is inherently unstable and compaction generates pulsed flow in waves as dilatancy is propagated upwards (Scott and Stevenson, 1984; McKenzie, 1985; Barcilon and Richter, 1986; Wiggins and Spiegelman, 1995). Heat advection by melt promotes a feedback relationship, so that prolate ellipsoidal waves or (sub-) vertical melt-filled channels may initiate from instabilities in the porosity structure (Connolly and Podladchikov, 1998); self-propagating melt-filled fractures may nucleate on these features (e.g. Rubin, 1995a), and are a condition for melt egress since porous flow of melt below the solidus is not feasible.

Such modelling yields realistic results for low-viscosity basalt melt flowing through mantle materials. In the crust, however, the viscosity of typical melts makes migration slow at low melt fractions (Brown *et al.*, 1995; Rutter and Neumann, 1995), even if revised estimates of viscosity based on more recent models are used in the calculations (Baker, 1996; Hess and Dingwell, 1996). In the analysis by McKenzie (1984), characteristic compaction lengths in the crust are small (see also Brown *et al.*, 1995; Rutter and Neuman, 1995), although these may be misleading (Connolly and Podladchikov, 1998). For these reasons, tectonic stresses are likely to be more important than buoyancy forces in melt extraction from partially-molten crustal protoliths, and in crustal systems, anisotropic permeability caused by variations in structure and lithology may be more important factors in controlling the flow and geometry of high-porosity domains.

Crustal-scale shear zone systems and fluid flow

Considerable evidence exists in nature for the structural control of fluid flow during regional metamorphism (Ferry, 1994b; Oliver, 1996), both by localization of strain during plastic deformation (Eisenlohr *et al.*, 1989; McCaig, 1997; Ord and Oliver, 1997) and by fracture channelization (Oliver *et al.*, 1993). The field observations are supported by modelling of processes in the metamorphic realm, which has been directed towards understanding focussed fluid flow and its consequences in response to regional stress gradients generated during active deformation of anisotropic crust (Ord, 1990; O'Hara, 1994; Connolly, 1997b; Ord and Oliver, 1997; Thompson, 1997; Koons *et al.*, 1998). Similar field evidence supports the view that movement of granite melt through partially-molten crust is structurally-controlled and driven by active deformation (Brown and Rushmer, 1997). Theoretical treatment based on experimental data underpins the necessity of such a relation (Rutter, 1997). If melt-enhanced embrittlement occurs, then melt may move along fracture pathways. Granular flow may be an important mechanism in the movement *en masse* of melt with residue, and in the segregation of melt from residue caused by differential rates of flow between melt and residue.

All geometric models of focussed fluid flow require extensive lateral migration of fluid (Connolly, 1997b; Cruden, 1998). This requirement is most pronounced for crustally-derived melts given the batholithic volumes of granite involved, which imply large source volumes. Thus, ascent of granite melt requires either substantial focussing by lateral flow into narrow channels over a large area of partially-molten source, or focussing of melt into narrow channels during *en masse* upward migration of a large volume of partially-molten crust.

Crustal-scale shear zone systems form percolation networks that focus fluid flow (O'Hara, 1994; McCaig, 1997; Ord and Oliver, 1997). Although the fluid-flow properties and the permeability structure of active shear zone systems are not adequately characterized, pervasive fluid flow probably occurs (Hobbs *et al.*, 1990; Ord, 1990; O'Hara, 1994; Tullis *et al.*, 1996;

McCaig, 1997; Ord and Oliver, 1997). Pervasive flow of crustally-derived melt can occur only above the solidus. We interpret the coincidence of foliation-parallel stromatic migmatite with concordant to weakly discordant granite sheets (Figs 2 & 3) in high strain zones within the CMB shear zone system to signify viscous flow of melt batches in sheet-like bodies either along foliation planes or at a shallow angle to the anisotropy, possibly in tensile and dilatant shear fractures. Flow is shown by asymmetric microstructures in sheets of schlieric granite (Fig. 4), and is to be expected in circumstances where pressure gradients are generated during active deformation of partially-molten anisotropic crust. It is implicit that the anatectic zone is permeable above the solidus, and that overpressuring and channelized flow have occurred. This suggests switches in effective permeability of the flow network may occur if overpressuring results in melt-enhanced embrittlement and fracturing in the source. Based on these observations and inferences, it is proposed that crustal-scale shear zone systems are the focussing mechanism by which melt is segregated and extracted from the source, and transferred to a crustal level where it can be emplaced as plutons in convergent orogens (D'Lemos *et al.*, 1992; Hutton, 1997; Brown and Solar, 1998).

DRIVING FORCES FOR MELT ASCENT

The driving force for melt ascent is often assumed to be buoyancy, and this is the driving force in both diapirism and dyking (Petford, 1996; Clemens *et al.*, 1997). For example, the buoyant ascent velocity of a spherical, isothermal diapir through isoviscous country rock can be approximated using Stokes' law, as follows

$$V = \frac{2\Delta\rho g r^2}{9\eta_{\mathrm{wr}}}, \tag{1}$$

where V is the terminal velocity, $\Delta\rho$ is the difference between the wall-rock density and the melt density, g is the acceleration due to gravity, r is the radius of the sphere, and η_{wr} is the kinematic viscosity of the wall rock (Mahon *et al.*, 1988). The critical parameter is the wall-rock viscosity, although diapirism is more efficient when power-law rheology is used in contrast to the Newtonian rheology used in equation (1) (Weinberg and Podladchikov, 1994). As Clemens *et al.* (1997) and others have pointed out, buoyant ascent of melt in a dyke of width w is powered by the same difference between the wall-rock density and melt density as in diapirism. Here, however, the factor that limits the vertical ascent velocity (V) is not wall-rock viscosity but the kinematic viscosity of the melt (η_{m}), as follows:

$$V = \frac{gw^2\Delta\rho}{12\eta_{\mathrm{m}}}. \tag{2}$$

To avoid arrest caused by crystallization during ascent through subsolidus crust, dykes need to grow to a critical minimum width within the source so that the flowing melt can advect heat faster than conduction through the dyke walls (Petford *et al.*, 1993; Rubin, 1993b, 1995b; Petford, 1996). As pointed out earlier, however, dyking *sensu stricto* is an inappropriate ascent mechanism during active contractional deformation. Also, for various reasons widely discussed in the literature (Petford, 1996; Weinberg, 1996; Clemens *et al.*, 1997), diapiric ascent is not thought to be the mechanism by which most granite has migrated through the crust, at least not through the upper crust.

Several authors have investigated the balance of forces that control melt fracture, melt migration and the geometric form of sheet intrusions, assuming elastic deformation of the host (Weertman, 1971; Pollard and Muller, 1976; Spence *et al.*, 1987; Emerman and Marrett, 1990; Lister, 1990; Lister and Kerr, 1991; Clemens and Mawer, 1992; Rubin, 1993c, 1995a). A discussion of the driving and resisting pressures during melt fracture of an elastically-deforming host, and the dominant physical balances between these pressures has been presented by Lister and Kerr (1991; see also Rubin 1995a), and particular examples are discussed by Reches and Fink (1988), Baer and Reches (1991) and Hogan and Gilbert (1995). Sleep (1988) has considered the tapping of melt by veins and dykes during viscous deformation and Rubin (1993a) has considered the issue of dykes vs diapirs in viscoelastic rock. In addition, at the crustal scale, Robin and Cruden (1994) have proposed that extrusion resulting from ductile transpression may help to drive upward migration of granite, and at the scale of the partially-molten source, Rutter (1997) has analyzed the driving forces for melt extraction during granular flow. Tectonic stresses and deformation of the crust are important controls, and we suggest that the balance of forces that drives melt migration may vary according to tectonic setting. These forces include: (1) buoyancy forces; (2) melt pressure; (3) extrusion pressure; (4) stresses related to the propagation of fractures; and (5) viscous pressure drop as a result of flow of magma in a fracture.

Driving forces for migration of granite during contractional deformation

For melt to segregate, a pressure gradient is necessary to drive melt flow in relation to the solid matrix (Sleep, 1988; Sawyer, 1994). This pressure gradient may originate in several ways, but ultimately it derives from some combination of buoyancy forces and tectonic stresses.

Buoyancy forces. The buoyancy forces acting on a body of melt are caused by a local difference between the gravitational forces acting on the melt and on the surrounding rocks (Lister and Kerr, 1991). This difference in gravitational force is equivalent to a hydrostatic pressure gradient on the melt given by:

$$\frac{dP}{dz} = (\rho_r - \rho_m)g \quad (3)$$

where ρ_r and ρ_m are the densities of rock and melt. If the density difference has a typical magnitude of $\Delta\rho$ during ascent, the total hydrostatic pressure is given by

$$\Delta P \sim \Delta\rho g h, \quad (4)$$

where h is the height of the rise. Although the resultant forces vary with depth and composition, for a typical $\Delta\rho$ of 300 kg m^{-3} [likely range of $\Delta\rho$ = 500–100 kg m^{-3} (Petford, 1996)] the pressure due to buoyancy generates a hydrostatic head up to ~100 MPa (Lister and Kerr, 1991), with a pressure gradient of up to $\sim 3.3 \times 10^{-3}$ MPa m^{-1} over a rise of ~30 km. For propagation of a dyke from a partially-molten source there must be excess pressure in the source (Lister and Kerr, 1991; Rubin, 1995a). The hydrostatic pressure appropriate to depth of formation can only be used if a batch of melt is connected both to the overpressured source and to a lower pressure sink higher in the crust. The rise of isolated volumes of melt has been analyzed by Secor and Pollard (1975). An isolated volume of melt of sufficiently large height may propagate upward, with an ascent velocity that increases as the size of the body increases (Rubin, 1995a). For a single fracture ~1 km in length in a ~20-km deep fracture system, Clemens and Mawer (1992) calculate that only ~5 km could be open by several meters because of infilling melt at any one time. This suggests that the flow of melt inflating a growing pluton is pulsed, consistent with the implications of a sheeted internal structure and the geochemistry of many granite plutons [the Phillips pluton, west-central Maine (Pressley and Brown, in press); cf. Barbero *et al*. (1995) and Krogstad and Walker (1996)]. It does mean, however, that the efficacy of hydrostatic pressure as a driving force for ascent is limited.

Melt pressure. There is no evidence that melt reaches vapor saturation at source depths in the crust, so that an internal increase in melt pressure caused by the large volume increase associated with bubble nucleation is not to be expected [except at the top of an extending melt-filled crack (Lister and Kerr, 1991)]. Ascending hydrous melt expands in response to decompression, however, producing a dilation pressure that increases with decreasing depth in the crust during ascent (Clemens and Mawer, 1992). The volume change of metamorphic reactions, ΔV_r, including melt-producing reactions, has been ascribed considerable importance for rock mechanics (Clemens and Mawer, 1992; Brown, 1994b). It has been argued that, because intermediate-to-low $a\mathrm{H_2O}$ melt-producing dehydration reactions involve positive ΔV_r, crustal anatexis under granulite facies conditions might be expected to generate internal melt pressure. Recently, it has been shown that in cases both of positive and negative ΔV_r, fluid pressure oscillates about the lithostat because of compactive processes (Connolly, 1997a). The primary factors generating fluid pressure are the connected porosity generated by the reduction in solid volume, the divergence of melt and rock pressure gradients within this porosity, *en masse* flow, and compaction (Sleep, 1988; Connolly, 1997a; Rutter, 1997).

Crustal anatexis and granite plutonism in orogenic belts are generally syntectonic processes (Blumenfeld and Bouchez, 1988; Karlstrom, 1989; Brown, 1994a; Benn *et al*., 1997; Hutton, 1997). Deformation of the anatectic zone, therefore, involves the compressibility behaviors of both the solid matrix and the melt-filled pores, and dilational deformation can be induced by changes in the internal melt pressure and the external applied stress. Changes in pore volume and porosity are important for melt flow, but changes in pore geometry in response to changes in the externally applied stress are not instantaneous, whereas pressurization of the melt is essentially immediate. This leads to the idea of effective stress (Terzaghi, 1925; Hubbert and Rubey, 1959; Hutton, 1997; Rutter, 1997), in which the effective normal stresses are reduced by an amount equal to the pore-melt pressure, and it provides the rationale behind the mechanism of melt (hydraulic) fracture (Secor, 1969; see also Phillips, 1972; Fyfe *et al*., 1978), and the accommodation of granular flow by melt-assisted diffusion creep (Rutter, 1997). Thus, melt pressure may lead to melt-enhanced embrittlement and failure by fracturing (Davidson *et al*., 1994). Whether or not embrittlement occurs to enhance melt flow is uncertain. The small overpressures required to permit deformation-propagated fluid flow by creep [< 50 MPa for metamorphic fluid flow (Connolly, 1997a), ~1 MPa for melt flow (Rutter, 1997)] suggest that embrittlement may not always happen.

Based on microstructural observations from dynamic melting experiments on granite (Rutter and Neumann, 1995; Rutter, 1997) and amphibolite (Rushmer, 1995, 1996; Brown and Rushmer, 1997), flow, *en masse*, of partially-molten rock involves cataclastic deformation of grains, granular flow between grains, and viscous flow of the melt. In these experiments, there was no evidence of deformation of grains by intracrystalline plasticity, and, in nature, flow *en masse* is expected to be accommodated by melt-enhanced diffusion creep (Dell'Angelo and Tullis, 1988). Migration *en masse* of melt plus residue (the 'magma mobility' of Sawyer, 1994), therefore, is likely to occur by granular flow accommodated by melt-enhanced diffusion creep, at a rate determined by the

rate of this accommodation. Calculations by Rutter (1997), using a modification of the model proposed by Paterson (1995), give strain rates $\sim 10^{-14}$ s^{-1} at 850°C for a grain size of 1 mm in a protolith with 0.3 wt% water, and yield a flow stress ~1 MPa. Additionally, Rutter (1997) estimates deformation-induced pressure gradients of ~1 MPa m^{-1} for distances ~1 m.

Extrusion pressure. Within a crustal-scale oblique-reverse shear zone system, such as the CMB shear zone system in west-central Maine, the orientation of the fabric anisotropy is inferred shallow in the contemporaneous lower–middle crust but steep in the contemporaneous upper–middle crust, which is now exposed at the Earth's surface (Brown and Solar, 1998). The geometry of such a system results in confined flow with extrusion of material upward through the system. Confined flow generates a gradient in the normal stress parallel to the zone that implies a pressure gradient decreasing in the direction of flow (Mancktelow, 1995a). This may be a significant driving force for extrusion of material in a reverse crustal-scale shear zone system (Mancktelow, 1995b). In addition, the steep part of the CMB shear zone system is analogous to models of vertical zones of symmetrical ductile transpression (Robin and Cruden, 1994; Tikoff and Teyssier, 1994; Thompson *et al*., 1997).

Ductile transpression implies extrusion of material up through the orogen, because the horizontal convergent pressure is partly transferred to a vertical extrusion force. The rate of exhumation is related to the rate of convergence and the inclination of the convergence vector (Robin and Cruden, 1994; Thompson *et al*., 1997). The pressure above lithostatic that develops at the bottom center of a ductile transpression zone can be estimated using the following expression (Jaeger, 1962, p. 142; Robin and Cruden, 1994, p. 462):

$$\Delta P \approx 1.5 \eta_c \phi Z_o^2, \tag{5}$$

where ΔP is the pressure above lithostatic, η_c is the kinematic viscosity of the crust, ϕ is the rate of shortening normal to the zone, and Z_o is the normalized height of the free erosion surface (z/h, where z = depth and h = half width of the zone, respectively). For ductile transpression zones of 5–50 km width and vertical extent of 25 km, if $\eta_c \sim 10^{20}$ Pas, and $\phi \sim 10^{-14}$ s^{-1}, then ΔP is ~150–1.5 MPa. This overpressure decreases with height in the ductile transpression zone. Generally, the development of a regional-scale ductile transpression zone is favored by high T, high pore fluid pressure and low viscosity (Robin and Cruden, 1994). As the crust begins to melt, ϕ will increase and η_c will decrease, and the anatectic zone will concentrate transpressive deformation.

Within the CMB shear zone system, strain was partitioned and localized into zones of higher and lower strain, which implies differences between these zones in viscosity and strain rate during deformation. These differences likely result in differences in extrusion pressure between zones of higher and lower strain accommodation, although with progressive melting and episodic melt loss the differences are difficult to estimate. Although the HSZs will be rheologically weaker below the solidus, above the solidus, the LSZs are characterized by inhomogeneous migmatites that are likely to have contained a higher melt fraction during the deformation than the stromatic migmatites. Thus, above the solidus, the LSZs become the rheologically weaker units. In these circumstances, material in the LSZ is driven upward through the shear zone system at a faster rate than the rheologically stronger material in the surrounding HSZs (Mancktelow, 1995b). Extrusion of partially-molten crust with moderate melt fraction will result in differential rates of flow for solid matrix and melt, enabling melt segregation (e.g. Sawyer, 1994).

Fracture extension and viscous pressure drop. For a discussion of stresses related to the dilation of melt fractures in a viscous matrix, the interested reader is referred to Sleep (1988). Lister and Kerr (1991), Clemens and Mawer (1992) and Rubin (1995a) consider the propagation of existing melt-filled fractures. The internal pressure required for the propagation of a melt-filled fracture is given by Lister and Kerr (1991) as:

$$\Delta P_f \sim \frac{K_c}{l^{1/2}}, \tag{6}$$

where K_c is the critical stress intensity factor, or fracture toughness, and l is the shorter of the two dimensions in the fracture plane.

The flow of melt in a sheet is driven by a spatial gradient ΔP_f in the fluid pressure P_f. According to Lister and Kerr (1991), the pressure drop ΔP_v in laminar flow along the length of a fracture may be estimated as:

$$\Delta P_v \sim \frac{\eta_m l^2}{w^2 t}, \tag{7}$$

where η_m is the kinematic viscosity of the melt, w is fracture width and t is the time since fracture initiation. If melt is in turbulent flow, this will be an underestimate of the viscous pressure drop (Lister and Kerr, 1991).

Conclusion

Buoyancy forces and tectonic stresses generate pressure gradients to drive melt flow relative to the solid matrix, which enables melt extraction during contractional deformation in convergent, especially transpressive orogens. Anisotropy of permeability depends on strain history, however, and other parameters, so that

flow paths are likely to be controlled by strain-induced anisotropies, such as foliation planes and mineral elongation lineations, and other factors such as crystallography, grain size and shape. Thus, percolative flow of melt is likely to be most effective during active deformation in shear zone systems, because the porosity is transient and the permeability is dynamic. Build-up of melt pressure, which depends on the relative rates of melt production and melt flow, may allow viscous flow to be channelized in sheet-like bodies. These sheet-like bodies may occupy fractures if build-up of melt pressure leads to melt-enhanced embrittlement; this would enable instantaneously pulsed egress of melt along the fractures. Volumetrically significant melt escape may occur more commonly late in the orogenic cycle, contemporaneous with peak metamorphism, either because porous flow becomes increasingly slow during waning deformation or because melt fraction increases faster than porous flow can drain the fluid from the system.

In the listric root of a reverse crustal-scale shear zone system, the orientation of strain-induced anisotropies are less favorable for effective upward migration of melt. In this circumstance, local differences in rheology within the rock mass and the requirements of strain compatibility mean that sites of lower pressure will be formed during deformation in response to applied differential stress. These sites may enable melt to flow across the anisotropy and migrate upward more effectively.

Ascent of melt by viscous flow as sheet-like bodies or in fractures is governed by the balance among buoyancy forces, hydrostatic pressure, melt pressure, melt rheology and viscous pressure drop. Other controls on the ascent of granite as sheets, however, will be similar to those that control ascent in dykes. Thus, continued ascent of granite sheets at temperatures and depths below the solidus will require a minimum sheet thickness (Petford *et al.*, 1993; Petford, 1996; Rubin, 1993b, 1995b). The shape and width of the sheet, and flow-rates will depend on the viscosity and the balance between the various driving and resistive pressures, including the regional stress regime (Pollard and Muller, 1976; Lister and Kerr, 1991). Viscous flow in the sheet is likely to be laminar (Petford, 1996).

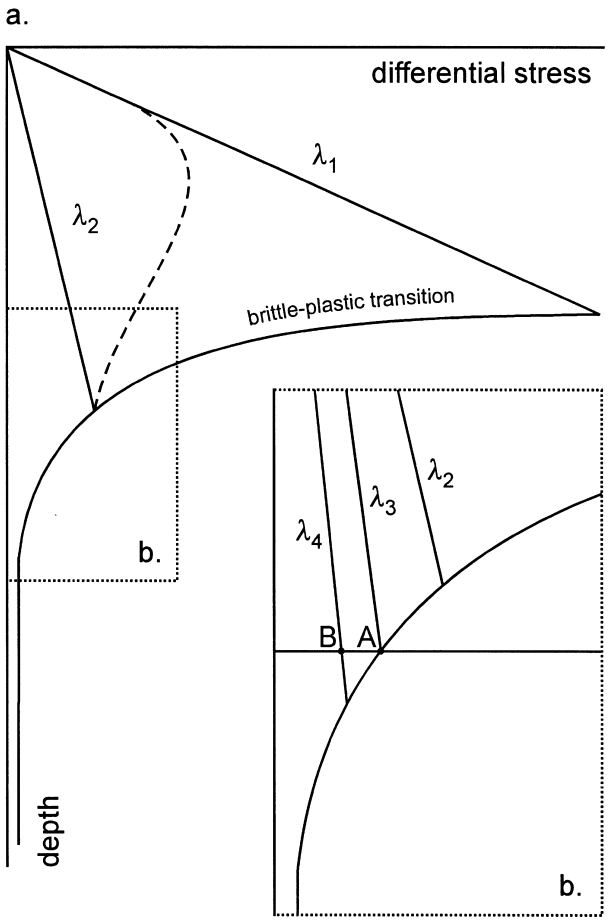

Fig. 6. (a) Schematic diagram of maximum differential stress versus depth for the Earth's crust in compression where the upper crust is dominated by brittle behavior and the lower crust by plastic flow. Values of differential stress outside the yield envelope are unstable. An increase in P_f (expressed in terms of λ_v, see text) decreases the brittle strength of the upper crust and extends the realm of brittle behavior to deeper levels. (b) The weaker nature of the upper crust is shown schematically by the dashed curve reflecting different values of λ_v. Melt-enhanced embrittlement occurs when partially-molten rocks, which are deforming plastically in response to an applied differential stress (e.g. at A) are intersected by the brittle strength curve (λ_3) as a result of an increase in melt pressure. For similar rocks subject to a lower applied differential stress (i.e. not flowing at a reasonable strain rate), higher melt pressure (λ_4) is needed for embrittlement to develop (e.g. at B). See text for further discussion.

CRUSTAL RHEOLOGY AND MELT-ENHANCED EMBRITTLEMENT

Crustal rheology

With decreasing depth in the crust, the differential stress required for flow at a given strain rate increases dramatically towards the brittle–plastic transition. This is illustrated schematically in Fig. 6, in which differential stress is plotted against depth. Yield envelopes for continental crustal rocks in compression vary as a function of composition, thermal structure, strain-rate and pore-fluid pressure. The yield envelope in Fig. 6 mimics those derived from experimental data on the rheology of wet quartzite, which has commonly been used as an analog for crustal rheology (Brace and Kohlstedt, 1980). Quartz rheology may be inappropriate during crustal anatexis that leaves mica-rich, mica + plagioclase-rich and plagioclase-rich residues, however, and we acknowledge that the rheology of other materials may be more suitable (e.g. mica schist, Shea and Kronenberg, 1992). In addition, a more complex model of crustal rheology, such as that proposed by Ord and Hobbs (1989), may ultimately be more appropriate.

In the model shown in Fig. 6, brittle–frictional processes are assumed in the upper crust and the differential stress–depth relation is linear, whereas thermally-activated crystal–plastic processes are generally assumed below the brittle–plastic transition, which give a power law rheology for the lower crust (e.g. Kirby, 1983). Temperature and pore-fluid pressure are the dominant factors that determine the rheological response of crustal rocks in compression, whereas order of magnitude changes in strain rate or difference in models of quartz rheology are secondary (Connolly, 1997a). Thus, for a particular thermal structure and fixed strain rate, the depth of the brittle–plastic transition is dependent only on the pore-fluid pressure (P_f) (Sibson, 1990).

Assuming fluid-saturation, the fluid pressure counteracts normal stresses (σ_n) according to the principle of effective stress, so that the effective normal stresses (σ'_n) are given by:

$$\sigma'_n = \sigma_n - P_f. \quad (8)$$

At a depth, z, in the crust, fluid pressure is conveniently defined by the pore-fluid factor (λ_v),

$$\lambda_v = P_f/\sigma_v = P_f/(\rho_r g z), \quad (9)$$

where σ_v is the vertical stress, ρ_r is average density of the rock column at depth z, and g is the acceleration due to gravity. Then, the effective overburden pressure (σ'_v) may be written,

$$\sigma'_v = \sigma_v - P_f = \rho_r g z(1 - \lambda_v), \quad (10)$$

so that the effective confining pressure on rock strength and ductility may be counteracted by increases in fluid pressure (Sibson, 1990). Thus, raising the pore-fluid pressure enables brittle behavior at lower differential stresses at any particular depth (compare the brittle strength for λ_2 with that for λ_1 in Fig. 6a). Above the solidus, the pore fluid is melt with a density in the range 2250–2450 kg m^{-3} (Clemens *et al.*, 1997), so that λ_v will be close to 1 in any case.

Assuming a hydrostatic pore-fluid pressure in the upper crust, then the brittle–plastic transition will occur at ~15 km depth for a geothermal gradient of ~25°C km^{-1}, and at shallower depths if the geothermal gradient is higher. Sibson (1974) has argued that the brittle–plastic transition is raised to shallower depths in the crust during compression, because of 'tectonic overpressure', and Koons and Craw (1991) have argued that concentration of rapid uplift in the inboard region of a convergent orogen produces a pronounced thermal anomaly that raises the brittle–plastic transition to within a few km of the surface. The crust between the anatectic zone and the brittle–plastic transition has a fluid-pressure gradient that oscillates close to lithostatic; thus, it will be weak, particularly during prograde metamorphism (Cox and Etheridge, 1989). According to Cox and Etheridge (1989), substantial regions in the crust may have flow behavior characterized by low strength and low stress and temperature sensitivities during deformation under prograde metamorphic conditions (shown schematically by the dashed curve in Fig. 6a); this may be a significant factor in enabling plastic deformation of the upper crust. These authors argue for a rheologically weak crust controlled by diffusive mass transfer processes beneath a shallow brittle–plastic transition zone and above the zone of deformation by intracrystalline plasticity. Significantly, partially-molten crust deforming by granular flow accommodated by melt-enhanced diffusion creep likely exhibits Newtonian viscosity, which would have significant implications for rheology of the lower crust and the tectonic behavior of convergent orogens (Wang *et al.*, 1994).

Melt-enhanced embrittlement

It has been argued that the presence of melt in the crust during deformation can lead to melt-enhanced embrittlement (Davidson *et al.*, 1994), and Roering *et al.* (1995) have argued for the presence of a low viscosity and low $a(H_2O)$ fluid to explain deep crustal embrittlement during granulite facies metamorphism. A conceptual model for melt-enhanced embrittlement has been developed by Davidson *et al.* (1994). In this model, conditions for failure are given by the combined Griffith [$\tau + 4\,T\sigma_n - 4\,T^2 = 0$, see Price and Cosgrove (1990, pp. 28–29)] and Navier–Coulomb [$\tau = 2\,T + \tan\phi\sigma_n$, see Price and Cosgrove (1990, pp. 28–29)] failure envelope on a Mohr diagram for stress (Fig. 7a).

In isotropic materials (Fig. 7a), tensile fractures form when σ_3 touches the failure envelope at A (at values of differential stress of $\sigma_1 - \sigma_3 < 4\,T$), dilatant shear fractures form in region B (at values of differential stress of $4\,T < \sigma_1 - \sigma_3 < 5.66\,T$), and compressional shear fractures form in region C (at values of differential stress of $\sigma_1 - \sigma_3 > 5.66\,T$) (Price and Cosgrove, 1990; Davidson *et al.*, 1994). During progressive melting of the crust, melt pressure increases and the effective normal stresses are reduced by an amount equal to the melt pressure until the Mohr circle touches the failure envelope. Under this condition, the partially-molten rock may fracture. If the Mohr circle touches the failure envelope in region B rather than at point A, then two potential orientations of dilatant shear fractures may form which have an acute angle of 2θ between them (Fig. 7a). The angle 2θ decreases with decreasing magnitude of the differential stress from a maximum of 45° when $(\sigma_1 - \sigma_3) = 5.66\,T$ to 0° when $(\sigma_1 - \sigma_3) = 4\,T$ (Price and Cosgrove, 1990). The orientation and spatial organization of melt fractures in the anatectic zone will be determined by the orientation of the principal stresses, the magnitude of the differential stress and the intrinsic properties of the partially-molten crustal materials. As a result, the expression of

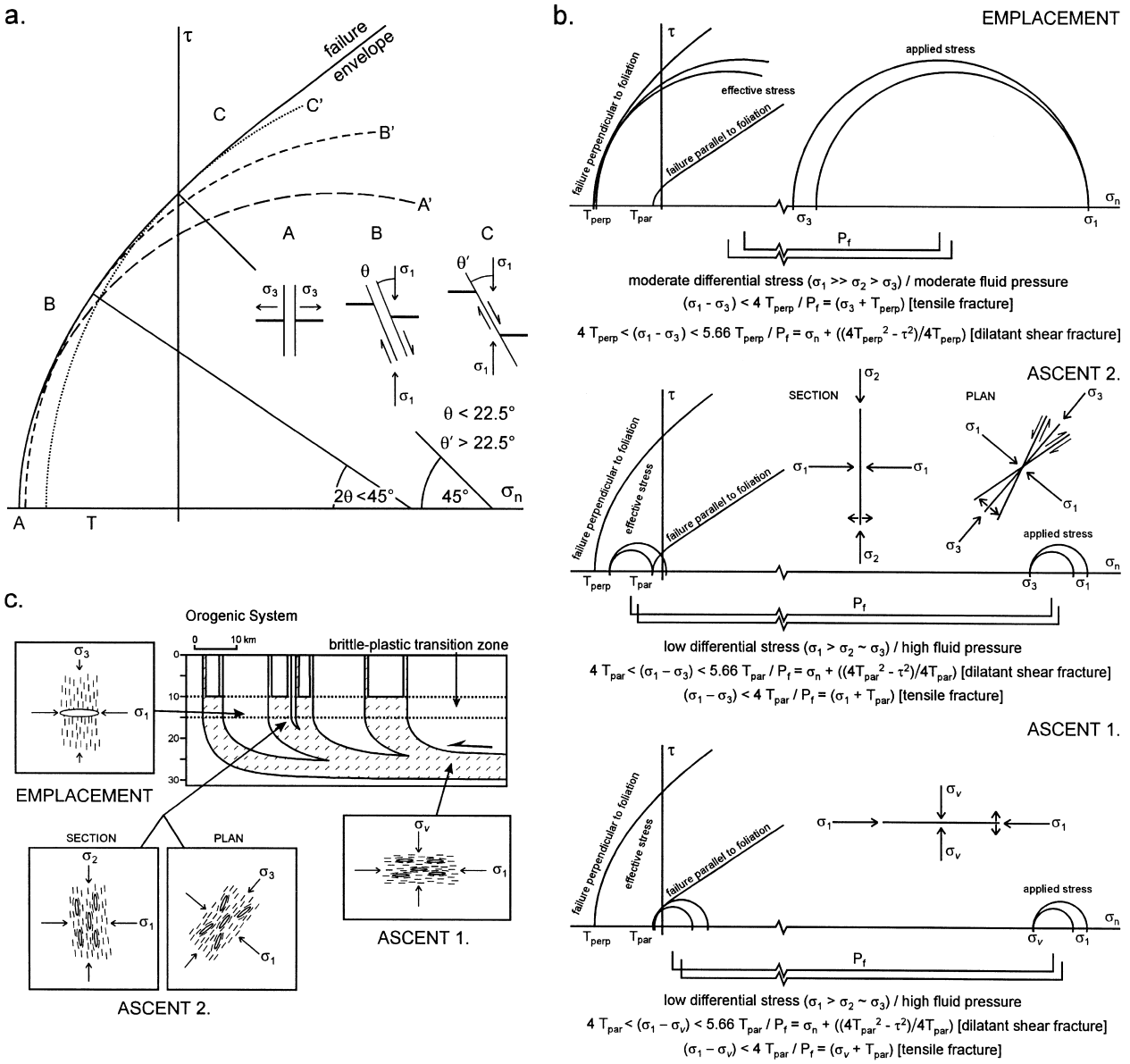

Fig. 7. (a) Mohr diagram for conditions of applied differential stress that will give rise to tensile failure at A, dilatant shear fractures in region B or compressional shear fractures in region C; three representative stress conditions are shown by the partial circles A′ (maximum applied differential stress for tensile failure), B′ (one example of the applied differential stress required for dilatant shear fracture) and C′ (minimum applied differential stress for compressional shear fracture). The sense of displacement exhibited by fracture planes and their orientation with respect to the axes of greatest and least principal stress are also shown. (b) Fracture orientations relative to rock fabric and principal compressional stresses in a strongly foliated rock with anisotropic tensile strength at three different levels within a crustal-scale shear zone system (see text for discussion). The trend of the fractures (lenses) relative to foliation and the principal compressional stresses is shown schematically in (c). In (c), inside the crustal-scale shear zone system, high strain zones are indicated by inclined dashes and low strain zones are unornamented. In (b), stress conditions for melt ascent are summarized in the bottom and middle diagrams (ASCENT 1 and ASCENT 2), and stress conditions for melt emplacement close to the brittle–plastic transition are summarized in the upper diagram (EMPLACEMENT) (see text for discussion).

melt fracturing may vary from conjugate shear fractures (e.g. Davidson *et al.*, 1994) to parallel tensile fractures (e.g. Lucas and St. Onge, 1995) to randomly-oriented tensile fractures and granular flow (e.g. Sawyer, 1998). Assuming other parameters are constant, the type of melt fracturing depends on decreasing flow stress with increasing melt fraction.

The rheological behavior of crustal materials is controlled by the intrinsic properties of the rock-forming minerals and the bulk properties of the rock mass, par-

ticularly its mechanical anisotropy. The mechanical anisotropy is determined by compositional layering, the interlayer properties such as the potential for interlayer slip and the alignment of minerals. The particular case considered herein deals with strongly-foliated rocks that were partially molten. One product is a stromatic migmatite in which the leucosome stromae are foliation-parallel. Consequently, at ambient P and T the partially-molten rock was highly anisotropic with a lower tensile strength normal to the anisotropy (Fyfe *et al*., 1978). As a result, there will be two end-member failure envelopes on a Mohr diagram for stress to represent the rheological behavior of a partially-molten rock, one that represents the stress conditions for failure along (parallel to) the layering/foliation, and another that represents the stress conditions for failure across (perpendicular to) the layering/foliation (Fig. 7b). Therefore, the orientation of fractures that may be generated in anisotropic materials, such as the crust when it is partially molten, is controlled by the difference in tensile strength along and normal to the anisotropy, the orientation of the layering/foliation with respect to the principal stresses, the magnitude of the applied stress, the magnitude of the differential stress, and the fluid pressure. These variations are illustrated schematically in Fig. 7 (b & c). The low strength expected for partially-molten crust is difficult to estimate, but the tensile strength normal to the anisotropy for failure parallel to layering in partially-molten rock is likely to be low, perhaps $\leq$1 MPa (Davidson *et al*., 1994). For rocks that are this weak, the differential stress cannot be large, and the vertical stress will be close to the horizontal stresses.

In partially-molten rocks that are deforming plastically, melt enhanced embrittlement may occur if melt pressure increases sufficiently to depress the brittle strength curve to the point that the differential stress is equal to the effective brittle strength of the partially-molten rock (Fig. 6b, λ_3 point A). In this condition, the partially-molten rocks may deform by plastic flow or may fracture as a result of melt-enhanced embrittlement. Thus, instantaneous changes in permeability may occur with increasing melt pressure if the mechanism of flow switches from porous flow to channelized flow. This leads to oscillatory behavior controlled by cyclic variations in λ_v, as melt pressure is moderated by pulsed egress of melt in sheet-like bodies, possibly channelized along fractures. It is suggested here that the stromatic migmatites in the HSZs of the CMB shear zone system are an example of such behavior. If similar partially-molten rocks are deforming plastically under some lower differential stress, then higher melt pressures are needed for embrittlement to occur (Fig. 6b, λ_4 point B). It is suggested here that an example of this behavior is provided by the inhomogeneous migmatites within the LSZs of the CMB shear zone system.

A MODEL FOR THE ASCENT AND EMPLACEMENT OF GRANITE DURING CONTRACTIONAL DEFORMATION, BASED ON THE WEST-CENTRAL MAINE CASE STUDY

Melt extraction and ascent

A plethora of studies shows that the first-order pattern of stresses in the lithosphere is largely the result of compressional forces applied at plate boundaries (Zoback, 1992, and references therein), and in active convergent orogens the maximum horizontal principal stress is at a high angle to the orogen; active extension is generally associated with high elevation as the vertical principal stress becomes σ_1 (Mercier *et al*., 1992). In ancient convergent orogens, structures indicate general shortening across the orogen, which suggests that a common system of stresses may be one in which σ_3 is (sub-) vertical and σ_1 is (sub-) horizontal and at a high angle to the strike of the orogen. Koons and Craw (1991; see also Koons, 1994) have argued that the inclination of σ_1 changes polarity from the outboard to the inboard side of convergent orogens, reflecting the change in dip of the topographic surface across the orogen (Koons, 1990; see also Koons, 1994). In obliquely convergent (transpressive) orogens, however, although σ_1 will be (sub-) horizontal, σ_3 need not necessarily be (sub-) vertical. Orogen-parallel extension (Brown and Talbot, 1989) suggests that another common system of stresses may be one in which σ_2 is (sub-) vertical. Whatever the orientation of the far-field principal stresses, local refraction of the stresses into orientations near parallel and perpendicular to the mechanical anisotropy may occur as a result of the presence of rheologically stronger layers. For the particular case considered herein, compositional layering and mineral fabrics are steep at outcrop and inferred to be shallow at deeper levels of the shear zone system, so that stress refraction will mean that the local principal stresses are likely to have been (sub-) vertical and (sub-) horizontal, except in the zone of curvature.

Foliated metamorphic rocks and stromatic migmatites are anisotropic with respect to strength, so that the orientation of the fabric will be important (Fyfe *et al*., 1978; Wickham, 1987; Shea and Kronenberg, 1993; Davidson *et al*., 1994; Lucas and St. Onge, 1995). For a system of stresses in the lower crust in which $\sigma_1 > \sigma_2 \sim \sigma_3$ with σ_2 or σ_3 (sub-) vertical, for fracture to occur along shallow fabrics (Fig. 7b, ascent 1) the fluid pressure must reduce the effective stress until the resolved normal stress across the fabric, approximated by the vertical principal stress (σ_v), is equal to the tensile strength normal to the anisotropy [T_{par}, where this is the tensile strength for failure along (parallel to) the fabric], i.e. $P_f = \sigma_v + T_{par}$. Conversely, for fracture to occur along steep fabrics (Fig. 7b, ascent 2) the fluid pressure generated must reduce the effective stress until

the resolved normal stress across the fabric, approximated by the maximum principal stress (σ_1), is equal to the tensile strength normal to the anisotropy (T_{par}), i.e. $P_f = \sigma_1 + T_{par}$. In both circumstances, the magnitude of the differential stress must be less than the difference in tensile strength along and normal to the anisotropy, otherwise fracture across (perpendicular to) the anisotropy will occur. If the condition occurs where the magnitude of the differential stress is equal to the difference in tensile strength, then there is an equal likelihood that both sets of fractures will form.

If the magnitude of the differential stress is less than the difference in tensile strength, as the volume of melt increases during crustal anatexis, failure will occur close to or along the anisotropy in the partially-molten rock (Fig. 7c), assuming that the local principal stresses are approximately perpendicular to, and within the plane of the anisotropy. With increasing melt fraction, the flow stress that can be supported decreases, which increases the likelihood that tensile fractures will show no preferred orientation (Cosgrove, 1995). Depending upon the magnitude of the differential stress, failure may occur by tensile fracture [shallow fabrics: $(\sigma_1 - \sigma_v) < 4\,T_{par}$, and $P_f = (\sigma_v + T_{par})$; steep fabrics: $(\sigma_1 - \sigma_3) < 4\,T_{par}$, and $P_f = (\sigma_1 + T_{par})$] or dilatant shear fracture [shallow fabrics: $(\sigma_1 - \sigma_v) > 4\,T_{par}$, but $< 5.66\,T_{par}$, and $P_f = \sigma_n + (4\,T_{par}^2 - \tau^2)/4\,T$; steep fabrics: $4\,T_{par} < (\sigma_1 - \sigma_3) < 5.66\,T_{par}$, $P_f = \sigma_n + (4\,T_{par}^2 - \tau^2)/4\,T$], where σ_v may be σ_2 or σ_3 (Price and Cosgrove, 1990; Davidson *et al.*, 1994).

In the lower crust, for circumstances in which the mechanical anisotropy is (sub-) horizontal, recalling the earlier discussion, if the magnitude of the differential stress is greater than the difference between the tensile strength along and normal to the anisotropy, then melt-enhanced embrittlement will lead to the formation of vertical tensile fractures. Alternatively, if the magnitude of the differential stress is less than the difference between the tensile strength along and normal to the anisotropy, then melt-enhanced embrittlement will lead to the formation of horizontal tensile fractures and/or weakly discordant dilatant shear fractures. Thus, depending on the magnitude of the differential stress, melt egress may occur by viscous flow in sheet-like bodies along the fabric or along weakly discordant dilational shear fractures, or in strongly discordant tensile fractures.

In partially-molten rock where rates of channelized flow greatly exceed rates of porous flow through the matrix, the matrix provides the storage porosity for pulsed flow in channels. The large fluid-pressure gradient between a fracture and the surrounding partially-molten rock promotes porous flow of melt into the fracture (Sleep, 1988). Porous flow [$v = -(k/\mu_m)dP/dX$, where v is the average velocity of melt, k is the permeability, μ_m is the viscosity of the melt and dP/dX is the pressure gradient] is driven by the effective pressure gradient, which depends on pressure drop and fracture spacing. The velocity of flow will depend on processes that control the permeability of the matrix and the kinematic viscosity of the fluid. Pressure gradients generated by fracturing will be short-lived, and the efficiency of melt flow into the fractures will depend on the magnitude of the stress drop (Wickham, 1987).

Zones of higher melt fraction are likely to have lower viscosity than zones of lower melt fraction; this means that zones of higher melt fraction exert a lower melt pressure, which may produce an instability in which melt is sucked into these zones (Stevenson, 1989). Rubin (1995a) has argued that such a process may be necessary to form channels in a partially-molten rock. These zones possess an internal melt pressure that is greater than the least principal compressive stress but less than the regional melt-pore pressure, so the zones may dilate by infiltrating melt. In an anisotropic material, in circumstances where σ_1 is parallel to the fabric anisotropy, the zones will dilate and extend in length. This is the situation in the listric root of the CMB shear zone system. As the zones dilate, melt pressure may cause embrittlement to enable fracture. An example may be the sheets of immigrant granite arrested during migration through the steeply-dipping stromatic migmatites (Figs 2 & 3). Melt extraction is a cyclic process, as shown by internal structure in the granites that suggests that sheet-like melt flow was pulsed, with multiple melt batches using the same pathways.

At temperatures below the solidus, strain is partitioned and localized into the rheologically weaker units that become the zones of higher strain. Above the solidus, however, the rheological properties are reversed, and the inhomogeneous migmatite of the LSZs becomes the rheologically weaker zone into which melt may flow. Strain continues to be localized into the HSZs, and the inhomogeneous migmatite of the LSZs is extruded through the system. As inhomogeneous migmatite is extruded through a crustal-scale shear zone system, granite melt segregates from residual matrix by granular-flow-induced compaction. Matrix compaction induces the elevation of melt pressure that is necessary to drive melt exfiltration from the system. In the model for granular flow accommodated by melt-enhanced diffusion creep (Rutter, 1997), deformation is expected to be compactive and stable, unless deformation of a weak matrix with a tendency for melt pressure to rise reduces the effective pressure such that granular flow becomes dilatant. Under this condition, localization of deformation into dilatant shear fractures or tensile fractures is likely to occur, and may be a necessary condition to expel melt from the system (Rutter, 1997; Brown and Solar, 1998). Exfiltration of melt lowers melt-pore pressure, so that granular flow again occurs in the shear-enhanced compaction regime. Thus, rapid switches in effective permeability of the flow network may occur and

exfiltration of melt from an extruding mass of inhomogeneous migmatite ascending by granular flow will be cyclic.

Conclusion

The overall model of melt extraction and ascent in a crustal-scale shear zone system involves creation of connected melt-filled porosity over a critical dip-length of the shear zone system. Percolative melt flow will occur along the fabric anisotropy, by taking advantage of the dynamic permeability produced during active deformation. In the listric root of reverse shear zone systems, however, melt may migrate upward by moving across the compositional layering and mineral fabrics using dilatant sites set up during heterogeneous deformation. Also, at low melt fraction the magnitude of the differential stress may exceed the difference between the tensile strength along and normal to the anisotropy, and vertical tensile fractures may contribute to melt migration across the compositional layering and mineral fabrics. During early evolution of the system, we expect that melt will be drained from deeper levels of the shear zone system. Build-up of melt pressure may enable migration by viscous flow as sheet-like bodies or in tensile and/or dilatant shear fractures; migration along the shear zone system is essentially controlled by the compositional layering and mineral fabrics. As the orogenic system evolves, deformation, metamorphism and anatexis progressively migrate to shallower levels and melt will be drained from shallower parts of the system. In west-central Maine, in both stromatic migmatites of the HSZs and inhomogeneous migmatites of the LSZs, melt extraction is cyclic, with porous flow followed by channelized melt egress. During this progressive evolution, an increasing volume of residual rocks is left behind.

Melt emplacement

In the case study area of west-central Maine, channelized flow of melt is inferred to be pulsed, based on the layered nature of the metre-scale granite sheets in the HSZs and the sheeted internal structure of the Phillips pluton. This raises the question of why and at what crustal level the first pulse of melt was arrested during ascent, and what was the critical rate of arrival of individual pulses to prevent freezing and allow lateral intrusion and pluton inflation. According to Clemens and Mawer (1992, p. 350), to construct a batholith of volume 2000 km^3 would require ~40 pulses of melt per year during an inflation period of *ca* 800 y, assuming a dyke of melt ~5 km in depth and ~12 m in average width ascending along a fracture ~1 km long in plan view. This volume is comparable to each of the Lexington and Mooselookmeguntic plutons. Depending upon the temperature at the level of emplacement and the melt temperature, plutons of this size likely take periods of one to two orders of magnitude longer than the inflation period to cool to the ambient temperature.

Within the CMB shear zone system, major structures and the fabric anisotropy are moderate-to-steeply dipping so that neither pre-existing (sub-) horizontal structures nor changes in lithology provide traps for melt accumulation and emplacement (Gretenner, 1969; Clemens and Mawer, 1992; Hogan and Gilbert, 1995). Although the major plutons in this area appear to have been emplaced around the level of the contemporary brittle–plastic transition, we do not envisage that this property of the crust will inhibit continued ascent of melt. The increasing level of supported differential stress with decreasing depth in the crust, however, favors a changeover to (sub-) horizontal fracture propagation (Fig. 7). Thus, if melt ascent becomes stalled, the melt may intrude laterally and inflate to form a horizontal tabular pluton.

We propose that melt ascent is stopped because the flow path intersects the solidus for the particular melt composition. This can be understood by reference to Fig. 8, which is a *P–T* diagram showing the water-saturated and dry solidi for muscovite granite, and the muscovite-dehydration and biotite-dehydration melting equilibria for quartzo–feldspathic assemblages (from Thompson, 1996). In their study of the Phillips pluton, Pressley and Brown (in press) concluded that the dominant leucogranite was derived by eutectic inter-

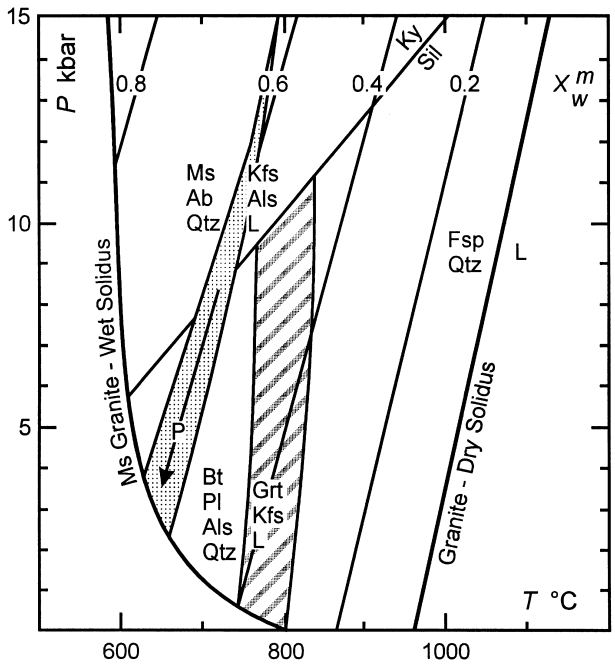

Fig. 8. *P–T* diagram showing the water-saturated (wet) and muscovite-dehydration melting (dry) solidi for a muscovite granite, with muscovite-dehydration and biotite-dehydration melting equilibria for quartzo–feldspathic assemblages relative to melting in the haplogranite system at decreasing X_w^m (after Thompson, 1996 and references therein). The arrow labeled P is a representative ascent path for leucogranite melt of the Phillips pluton. Symbols for rock-forming minerals after Kretz (1983).

mediate $a(H_2O)$ muscovite-dehydration melting of a pelite source similar to those exposed in the Central Maine Belt. Given the geometry of the CMB shear zone system, we expect that these melts were derived from depths of around 25 km, or 700–800 MPa at 700–720°C (Fig. 8). The decompression path for melt in P–T space will depend on the rate of ascent, and this path will determine whether entrained residue is resorbed or phenocrysts are crystallized during ascent (Holtz and Johannes, 1994; Clemens *et al.*, 1997). For this discussion, an ascent path of constant X_w^m is assumed, so that minerals are neither resorbed nor crystallized (Fig. 8, arrow labeled P). This means that the ascent path will intersect the water-saturated solidus for muscovite granite at depths corresponding to pressures of 400–200 MPa (Fig. 8).

How does this relate to emplacement? The first few melt pulses may crystallize and block further ascent, but given the rate at which individual pulses of melt are expected to arrive (e.g. ~40 pulses of melt per year during an inflation period of *ca* 800 y, see earlier discussion), the accumulation of melt will inhibit fast cooling and raise melt pressure to a sufficient level that (sub-) horizontal fracture may occur (Fig. 7c). Depending upon the value of the differential stress, $\sigma_1-\sigma_3$, failure may occur by tensile fracture [$\sigma_1-\sigma_3 < 4\,T_{perp}$, and $P_f > (\sigma_3 + T_{perp})$] or dilatant shear fracture [$4\,T_{perp} < \sigma_1-\sigma_3 < 5.66\,T_{perp}$, and $\sigma_3 < P_f < (\sigma_3 + T_{perp})$, where T_{perp} is the tensile strength for failure across (perpendicular to) the fabric].

Once formed, a horizontal sheet can inflate if sufficient melt pressure is available (e.g. Johnson, 1970; Corry, 1988). Inflation from sheet to pluton generally requires lifting of the roof or sinking of the floor (Cruden, 1998). Most studies consider lifting of the roof to form a laccolith to be a shallow level phenomenon, with all documented examples occurring at palaeodepths <3 km and pluton growth that rarely exceeds 2 km in thickness (Corry, 1988). With increasing overburden thickness, (sub-) horizontal fracture propagation and lateral growth are favored over roof lifting and vertical growth so that the aspect ratio of laccoliths increases with depth (Roman-Berdiel *et al.*, 1995). At greater depths, sinking of the floor during intrusion likely occurs and lopoliths form (Cruden, 1998). This is consistent with models of the three-dimensional form of plutons based on gravity data that suggest inwardly-inclined pluton floors and geometric similarity to lopoliths (e.g. Vigneresse, 1988, 1990, 1995). Inflation by sinking of the floor requires accommodation in the underlying crust, most likely by complementary volume loss at depth as a result of extraction of melt. In effect, this is crustal-scale convection (Zen, 1995; Weinberg, 1997), and the mass balance is achieved by distributed flow rather than through local accommodation. The exact mechanism by which this is accomplished might be expected to vary with depth, so that the end-member models investigated by Cruden (1998) of piston sinking and cantilever mechanisms might reflect increasing depth. It is likely that strain is accommodated by a feedback relation in which transfer of granite melt from the anatectic domain to the upper crust allows pluton inflation by sinking of the floor and distributed return flow (Cruden, 1998).

In west-central Maine, pluton emplacement was close to the contemporaneous brittle–plastic transition, so that inflation of the plutons by subsidence of the floor is more likely to have been accommodated by the cantilever mechanism of Cruden (in press) rather than the piston sinking mechanism. Possible examples of pluton inflation by subsidence of the floor in west-central Maine are the Redington and Mooselookmeguntic plutons. Additionally, (sub-) vertical stretching across HSZs within the CMB shear zone system may have helped in creation of space to ease inflation of the Lexington pluton.

DISCUSSION: OROGENIC SYSTEMS

Although the search for a minimal set of principles to describe granite ascent and emplacement is consistent with the normal methodology of science, many natural systems are dynamic and far from equilibrium so that self-organized criticality may be a more appropriate paradigm. The synchronous nature of deformation, metamorphism and plutonism in convergent orogens and the large array of interrelated factors that control granite ascent and emplacement suggest the operation of multiple feedback relations (Brown and Solar, 1998). Orogenic belts are complex systems that evolve dynamically into a critical state without external tuning—it is this feature that leads to amplification of initial fluctuations in feedback relations, and development of dissipative structure through self-organization into shear zone systems (Brown and Solar, 1998). Expression of self-organization occurs on a time-scale less than that of the orogenic system, and on a length-scale accommodated by the orogenic system. In the west-central Maine case study, the time-scale was several million years and the length-scale, tens of kilometers. In anisotropic crustal materials, the orientation of the anisotropy is an important control on melt flow paths. Thus, in anatectic domains within the orogenic system, stromatic migmatites may be characteristic of HSZs, to suggest percolative flow along the migmatite fabric, and inhomogeneous migmatites may be characteristic of LSZs, to suggest granular flow parallel to the mineral elongation lineation. Channelized flow is represented by granite sheets, which may be emplaced in tensile and dilatant shear fractures. These features record elements of the dissipative process.

Within an orogenic system, internal compartments are formed separated by impermeable seals. An example is the compartment defined by the bounding

surfaces of the crustal-scale shear zone system and the brittle–plastic transition (Fig. 5, the contemporary brittle–plastic transition was around the present level of erosion; see also Fig. 7c), within which LSZs represent internal compartments sealed by HSZs. If compartments within the system or the system as a whole become overpressured, melt is expelled either by viscous flow as sheet-like bodies or along fractures (tensile fracture and/or dilatant shear fractures at a high angle to σ_1), which is likely to be an episodic feature. Thus, we expect granite plutons to overlie ascent conduits that link downward, along the mineral elongation lineation, to inhomogeneous migmatite in LSZs, although lateral expansion during intrusion and inflation may mean that some plutons extend beyond the limits of the parental LSZ. This cyclic process has been called dilatancy-driven fluid pumping (Brown, 1994a). Fugitive melt ponds in plutons because the solidus is approached with decreasing P stalling ascent. For intermediate $a(H_2O)$ muscovite-dehydration melting, the flow path intersects the solidus around the level where the increasing supported differential stress favors failure by fracturing at a high angle to the plane of ascent (tensile fracture and/or dilatant shear fractures at a low angle to σ_1). In convergent orogens characterized by steep fabrics, these horizontal tabular plutons may have discordant relations with the country rock structures, yet at the crustal-scale they are syn-tectonic.

Acknowledgements—We thank the conveners of the Symposium sponsored by the GAC Structural Geology and Tectonics Division on 'Extraction, Transport, and Emplacement of Granitic Magmas: Physical Processes and Structural Signatures' for the opportunity to present this work as part of the Symposium. We acknowledge helpful discussions on the regional geology of west-central Maine with many people, including Tim Allen, Spike Berry, Jack Cheney, Tom Foster, Chuck Guidotti, Mike Holdaway, Bob Marvinney, Bob Moench, Rachel Pressley, Dave Stewart, Paul Tomascak and E-an Zen. Several colleagues provided preprints of work in review or in press, including Jamie Connolly, Sandy Cruden, Mike Holdaway, Scott Paterson and Ed Sawyer. We thank Sandy Cruden, Mary Hubbard, Scott Paterson, Ed Sawyer, Mike Williams and E-an Zen for constructive criticism and corrections. Scott Paterson has striven to keep us honest and Ernie Rutter has tried to educate the senior author in rock mechanics. Nonetheless, remaining misperceptions are our responsibility. We regret we cannot yet answer all of the questions asked of us by reviewers, and we continue to strive for greater insight. We acknowledge partial support of this work from the Department of Geology, University of Maryland, the Geological Society of America Research Grants Program and NSF Grant EAR-9705858. We thank Jeanne Martin for skilled word processing support and her tolerance of the senior author.

REFERENCES

Anderson, E. M. (1938) The dynamics of sheet intrusion. *Proceedings of the Royal Society of Edinburgh* **58,** 242–251.

Anderson, E. M. (1951) *The Dynamics of Faulting and Dyke Formation With Application to Britain*. Oliver and Boyd, London.

Baer, G. and Reches, Z. (1991) Mechanics of emplacement and tectonic implications of the Ramon Dyke Systems, Israel. *Journal of Geophysical Research* **96,** 11895–11910.

Baker, D. R. (1996) Granite melt viscosities: Empirical and configurational entropy models for their calculation. *American Mineralogist* **81,** 126–134.

Barbero, L., Villaseca, C., Rogers, G. and Brown, P. E. (1995) Geochemical and isotopic disequilibrium in crustal melting: An insight from the anatectic granitoids from Toledo, Spain. *Journal of Geophysical Research* **100,** 15 745–15 765.

Barcilon, V. and Richter, F. M. (1986) Non-linear waves in compacting media. *Journal of Fluid Mechanics* **164,** 429–448.

Batt, G. E. and Braun, J. (1997) On the thermo-mechanical evolution of compressional orogens. *Geophysical Journal International* **128,** 364–382.

Benn, K., Horne, R. J., Kontak, D. J., Pignotta, G. S. and Evans, N. G. (1997) Syn-Acadian emplacement model for the South Mountain batholith, Meguma Terrane, Nova Scotia: magnetic fabric and structural analyses. *Geological Society of America Bulletin* **109,** 1279–1293.

Blumenfeld, P. and Bouchez, J. L. (1988) Shear criteria in granite and migmatite deformed in the magmatic and solid states. *Journal of Structural Geology* **10,** 361–372.

Brace, W. F. and Kohlstedt, D. L. (1980) Limits on lithospheric stress imposed by laboratory experiments. *Journal of Geophysical Research* **85,** 6248–6252.

Bradley, D., Tucker, R. D. and Lux, D. (1996) Early Emsian position of the Acadian orogenic front in Maine. *Geological Society of America Annual Meeting, Abstracts with programs* **28,** A–500.

Brantley, S. L., Fisher, D. M., Deines, P., Clark, M. B. and Myers, G. (1997) Segregation veins: evidence for the deformation and dewatering of a low-grade metapelite. In *Deformation-Enhanced Melt Segregation and Metamorphic Fluid Transport*, ed. M. Holness, pp. 267–288. The Mineralogical Society Series, Chapman and Hall, London, **8**.

Brown, E. H. and Talbot, J. L. (1989) Orogen-parallel extension in the North Cascades Crystalline Core, Washington. *Tectonics* **8,** 1105–1114.

Brown, M. (1994a) The generation, segregation, ascent and emplacement of granite magma: The migmatite-to-crustally-derived granite connection in thickened orogens. *Earth-Science Reviews* **36,** 83–130.

Brown, M. (1994b) Melt segregation mechanism controls on the geochemistry of crustal melts. *V.M. Goldschmidt Conference, Mineralogical Magazine* **58A,** 124–125.

Brown, M. (1995) Late-Precambrian geodynamic evolution of the Armorican Segment of the Cadomian Belt (France): Distortion of an active continental margin during south-west directed convergence and subduction of a bathymetric high. *Géologie de la France* **3,** 3–22.

Brown, M. A. and Brown, M. (1997) What is the connectivity of melt in the anatectic zone? Problems and Approaches. *Geological Society of America, Abstracts with Programs* **29,** A–91.

Brown, M. and Dallmeyer, R. D. (1996) Rapid Variscan exhumation and role of magma in core complex formation: Southern Brittany metamorphic belt, France. *Journal of Metamorphic Geology* **14,** 361–379.

Brown, M. and Rushmer, T. (1997) The role of deformation in the movement of granitic melt: Views from the laboratory and the field. In *Deformation-enhanced Melt Segregation and Metamorphic Fluid Transport*, ed. M. Holness, pp. 111–144. The Mineralogical Society Series, Chapman and Hall, London, **8**.

Brown, M. and Solar, G. S. (1998) Shear zones and melts: positive feedback in orogenic belts. *Journal of Structural Geology* **20,** 211–227.

Brown, M., Averkin, Y., McLellan, E. and Sawyer, E. (1995) Melt segregation in migmatites. *Journal of Geophysical Research* **100,** 15 655–15 679.

Carnese, M. J. (1981) Gravity study of intrusive rocks in west-central Maine. M.Sc. thesis. University of New Hampshire, .

Clemens, J. D. and Mawer, C. K. (1992) Granitic magma transport by fracture propagation. *Tectonophysics* **204,** 339–360.

Clemens, J. D., Petford, N. and Mawer, C. K. (1997) Ascent mechanisms of granitic magmas: Causes and consequences. In *Deformation-Enhanced Fluid Transport in the Earth's Crust and Mantle*, ed. M. B. Holness. The Mineralogical Society Series, Chapman and Hall, London, **8**.

Collins, W. J. and Sawyer, E. W. (1996) Pervasive granitoid magma transfer through the lower–middle crust during non-coaxial com-

pressional deformation. *Journal of Metamorphic Geology* **14,** 565–579.
Connolly, J. A. D. (1997a) Devolatilization-generated fluid pressure and deformation-propagated fluid flow during prograde regional metamorphism. *Journal of Geophysical Research* **102,** 18 149–18 173.
Connolly, J. A. D. (1997b) Mid-crustal focused fluid movement: thermal consequences and silica transport. In *Fluid Flow and Transport in Rocks*, eds B. Jamtveit and B. W. D. Yardley, pp. 235–250. Chapman and Hall, London.
Connolly, J. A. D. and Podladchikov, Y. U. (in press) Compaction-driven fluid flow in viscoelastic rock. *Geodynamica Acta*.
Corry, C. E. (1988) *Laccoliths: Mechanics of Emplacement and Growth*. Geological Society of America, Special Publication.
Cosgrove, J. W. (1995) The expression of hydraulic fracturing in rocks and sediments. In *Fractography: Fracture Topography as a Tool in Fracture Mechanics and Stress Analysis*, ed. M. S. Ameen, pp. 187–196. Geological Society Special Publication, **92**.
Cox, S. F. and Etheridge, M. A. (1989) Coupled grain-scale dilatancy and mass transfer during deformation at high fluid pressures: Examples from Mt. Lyell, Tasmania. *Journal of Structural Geology* **11,** 147–162.
Cruden, A. R. (1998) On the emplacement of tabular granites. *Journal of the Geological Society, London* **154,** 853–862.
Cruden, A. R. and Launeau, P. (1994) Structure, magnetic fabric and emplacement of the Archean Lebel Stock, SW Abitibi Greenstone Belt. *Journal of Structural Geology* **16,** 677–691.
Cruden, A. R. and Robin, P-Y. F. (1997) *Low Viscosity Shear Zones Within Broader Ductile Transpression Zones. Part II: Analog Models*. Abstract, Canadian Tectonics Group AGM, Halifax.
Davidson, C., Hollister, L. S. and Schmid, S. M. (1992) Role of melt in the formation of a deep-crustal compressive shear zone: The MacLaren Glassier metamorphic belt, south-central Alaska. *Tectonics* **11,** 348–359.
Davidson, C., Schmid, S. M. and Hollister, L. S. (1994) Role of melt during deformation in the deep crust. *TERRA Nova* **6,** 133–142.
Dell, Angelo L. N. and Tullis, J. (1988) Experimental deformation of partially melted granitic aggregates. *Journal of Metamorphic Geology* **6,** 495–516.
Dickerson, R. P. and Holdaway, M. J. (1989) Acadian metamorphism associated with the Lexington batholith, Bingham, Maine. *American Journal of Science* **289,** 945–974.
D'Lemos, R. S., Brown, M. and Strachan, R. A. (1992) Granite magma generation, ascent and emplacement within a transpressional orogen. *Journal of the Geological Society, London* **149,** 487–490.
Eisenlohr, B. N., Groves, D. and Partington, G. A. (1989) Crustal-scale shear zones and their significance to Archean gold mineralization in Western Australia. *Mineralum Deposita* **24,** 1–8.
Emerman, S. H. and Marrett, R. (1990) Why dykes? *Geology* **18,** 231–233.
England, P. C. and Thompson, A. B. (1984) Pressure–temperature–time paths of regional metamorphism I. Heat transfer during the evolution of regions of thickened continental crust. *Journal of Petrology* **25,** 894–928.
Etheridge, M. A., Wall, V. J. and Cox, S. F. (1984) High fluid pressures during regional metamorphism and deformation: implications for mass transport and deformation mechanisms. *Journal of Geophysical Research* **89,** 4344–4358.
Eusden, J. D., Jr and Barreiro, B. (1988) The timing of peak high-grade metamorphism in central-eastern New England. *Maritime Sedimentation and Atlantic Geology* **24,** 241–255.
Ferry, J. M. (1994a) A historical review of metamorphic fluid flow. *Journal of Geophysical Research* **99,** 15487–15498.
Ferry, J. M. (1994b) Overview of the petrologic record of fluid flow during regional metamorphism in northern New England. *American Journal of Science* **294,** 905–988.
Fyfe, W. S., Price, N. J. and Thompson, A. B. (1978) *Fluids in the Earth's Crust*. Elsevier, The Netherlands.
Gaudette, H. E. and Boone, G. M. (1985) Isotope age of the Lexington Batholith, constraints on timing of intrusion and Acadian metamorphism in western Maine. *Geological Society of America, Abstracts with Programs* **17,** 19–20.
Gavrilenko, P. and Geugen, Y. (1993) Fluid overpressures and pressure solution in the crust. *Tectonophysics* **217,** 91–110.
Gretener, P. E. (1969) On the mechanics of the intrusion of sills. *Canadian Journal of Earth Sciences* **6,** 1415–1419.
Guidotti, C. V. (1974) Transition from staurolite to sillimanite zone, Rangeley Quadrangle, Maine. *Geological Society of America Bulletin* **85,** 475–490.
Guidotti, C. V. (1989) Metamorphism in Maine: an overview. In *Studies in Maine Geology, Volume 3: Igneous and Metamorphic Geology*, eds R. D. Tucker and R. G. Marvinney, pp. 1–19. Maine Geological Survey, Maine Department of Conservation.
Guidotti, C. V. (1993) Textural aspects of high *T*–low *P* polymetamorphism in the Rangeley Area, western Maine: General implications for studies of Acadian metamorphic rocks in New England. *Geological Society of America, Abstracts with Programs* **25**(2), A–21.
Guidotti, C. V. and Holdaway, M. J. (1993). Petrology and field relations of successive metamorphic events in pelites of west-central Maine. In *Fieldtrip Guidebook for the Northeastern United States*. eds J. T. Cheney and J. C. Hepburn. Geological Society of America. pp. L1–L26.
Guidotti, C. V., Teichmann, F. and Henry, D. J. (1991) Chlorite-bearing polymetamorphic metapelites in the Rangeley Area, Maine. *American Mineralogist* **76,** 867–879.
Hatch, N. L., Jr, Moench, R. H. and Lyons, J. B. (1983) Silurian–lower Devonian stratigraphy of eastern and south-central New Hampshire: Extensions from western Maine. *American Journal of Science* **283,** 739–761.
Hess, K.-U. and Dingwell, D. B. (1996) Viscosities of hydrous leucogranitic melts: A non-Arrhenian model. *American Mineralogist* **81,** 1297–1300.
Hobbs, B. E., Mühlhaus, H-B. and Ord, A. (1990) Instability, softening and localization of deformation. In *Deformation Mechanisms, Rheology and Tectonics*, eds R. J. Knipe and E. H. Rutter, pp. 143–165. Geological Society Special Publication, **54**.
Hogan, J. P. and Gilbert, M. C. (1995) The A-type Mount Scott Granite sheet: Importance of crustal magma traps. *Journal of Geophysical Research* **100,** 15 779–15 792.
Holdaway, M. J. and Mukhopadhyay, B. (1996) Redetermination of garnet and biotite margules parameters and recalibration of the garnet–biotite geothermometer and the muscovite–almandine–biotite–sillimanite (MABS) geobarometer. *Geological Society of America Annual Meeting, Abstracts with programs* **28,** A–356.
Hollister, L. S. and Crawford, M. L. (1986) Melt-enhanced deformation: A major tectonic process. *Geology* **14,** 558–561.
Holness, M. B. (1997) The permeability of non-deforming rock. In *Deformation-Enhanced Melt Segregation and Metamorphic Fluid Transport*, ed. M. Holness, pp. 9–39. The Mineralogical Society Series, Chapman and Hall, London, **8**.
Holtz, F. and Johannes, W. (1994) Maximum and minimum water contents of granitic melts—implication for chemical and physical properties of ascending magmas. *Lithos* **32,** 149–159.
Hubbert, M. K. and Rubey, W. W. (1959) Role of fluid pressure in mechanics of overthrust faulting. I. Mechanics of fluid-filled porous solids and its application to overthrust faulting. *Geological Society of America Bulletin* **70,** 115–166.
Huerta, A. D., Royden, L. H. and Hodges, K. V. (1996) The interdependence of deformation and thermal processes in mountain belts. *Science* **273,** 637–639.
Hutton, D. H. W. (1997) Syntectonic granites and the principle of effective stress: A general solution to the space problem? In *Granite: From Segregation of Melt to Emplacement Fabrics*, eds J. L. Bouchez, D. H. W. Hutton and W. E. Stephens, pp. 189–197. Kluwer Academic Publishers, The Netherlands.
Jaeger, J. C. (1962) *Elasticity, Fracture and Flow*. John Wiley & Sons, New York.
Jamieson, R. A., Beaumont, C., Hamilton, J. and Fullsack, P. (1996) Tectonic assembly of inverted metamorphic sequences. *Geology* **24,** 839–842.
Jamieson, R. A., Beaumont, C., Fullsack, P. and Lee, B. (1998) Barrovian regional metamorphism: Where's the heat? In *What Controls Metamorphism and Metamorphic Reactions?*, eds P. J. Treloar and P. J. O'Brien, pp. 23–51. Geological Society Special Publication, **138**.
Johnson, A. M. (1970) *Physical Processes in Geology*. Freeman, Cooper and Company, San Francisco.
Jones, K. A. and Brown, M. (1990) High-temperature 'clockwise' *P*–*T* paths and melting in the development of regional migmatites: an example from southern Brittany, France. *Journal of Metamorphic Geology* **8,** 551–578.

Karlstrom, K. E. (1989) Toward a syntectonic paradigm for granitoids. *Eos, Transactions of the American Geophysical Union* **70,** 762–763.

Kirby, S. H. (1983) Rheology of the lithosphere. *Reviews of Geophysics and Space Physics* **21,** 1458–1487.

Knipe, R. J. and McCaig, A. N. (1994) Microstructural and microchemical consequences of fluid flow in deforming rocks. In *Geofluids: Origin, Migration and Evolution of Fluids in Sedimentary Basin*, ed. J. Parnell, pp. 99–111. Geological Society Special Publication, **78**.

Koons, P. O. (1990) Two-sided orogen: collision and erosion from the sandbox to the Southern Alps, New Zealand. *Geology* **18,** 679–682.

Koons, P. O. (1994) 3-Dimensional critical wedges: Tectonics and topography in oblique collisional orogens. *Journal of Geophysical Research* **99,** 12301–12315.

Koons, P. O. and Craw, D. (1991) Evolution of fluid driving forces and composition within collisional orogens. *Geophysical Research Letters* **18,** 935–938.

Koons, P. O., Craw, D., Cox, S. C., Upton, P., Templeton, A. S. and Chamberlain, C. P. (1998) Fluid flow during active oblique convergence: A Southern Alps model from mechanical and geochemical observations. *Geology* **26,** 159–162.

Kretz, R. (1983) Symbols for rock-forming minerals. *American Mineralogist* **68,** 277–279.

Krogstad, E. J. and Walker, R. J. (1996) Evidence of heterogeneous crustal sources: the Harney Peak Granite, South Dakota, U.S.A. *Transactions of the Royal Society of Edinburgh: Earth Sciences* **87,** 331–337.

Laporte, D. and Watson, E. B. (1995) Experimental and theoretical constraints on melt distribution in crustal sources: The effect of crystalline anisotropy on melt interconnectivity. *Chemical Geology* **124,** 161–184.

Laporte, D., Rapaille, C. and Provost, A. (1997) Wetting angles, equilibrium melt geometry, and the permeability threshold of partially molten crustal protoliths. In *Granite: From Melt Segregation to Emplacement Fabrics*, eds J. L. Bouchez, D. Hutton and W. E. Stephens, pp. 31–54. Kluwer Academic Publishers, The Netherlands.

Lister, J. R. (1990) Buoyancy-driven fluid fracture: Similarity solutions for the horizontal and vertical propagation of fluid-filled cracks. *Journal of Fluid Mechanics* **217,** 213–239.

Lister, J. R. and Kerr, R. C. (1991) Fluid–mechanical models of crack propagation and their application to magma transport in dykes. *Journal of Geophysical Research* **96,** 10049–10077.

Lucas, S. B. and St. Onge, M. (1995) Syn-tectonic magmatism and the development of compositional layering, Ungava Orogen (northern Quebec, Canada). *Journal of Structural Geology* **17,** 475–491.

Mahon, K. I., Harrison, T. M. and Drew, D. A. (1988) Ascent of a granitoid diapir in a temperature varying medium. *Journal of Geophysical Research* **93,** 1174–1188.

Mancktelow, N. S. (1995a) Deviatoric stress and the interplay between deformation and metamorphism. *Geological Society of Australia, Abstracts, Clare Valley Conference* **40,** 95–96.

Mancktelow, N. S. (1995b) Nonlithostatic pressure during sediment subduction and the development and exhumation of high-pressure metamorphic rocks. *Journal of Geophysical Research* **100,** 571–583.

Marsh, B. D. (1982) On the mechanics of igneous diapirism, stoping, and zone melting. *American Journal of Science* **282,** 808–855.

Mawer, C. K., Clemens, J. D., Petford, N. D., Warren, R. G. and Ellis, D. J. (1997) Mantle underplating, granite tectonics, and metamorphic *P–T–t* paths: comment and reply. *Geology* **25,** 763–765.

McCaffrey, K. J. W. and Petford, N. (1997) Are granitic intrusions scale invariant? *Journal of the Geological Society, London* **154,** 1–4.

McCaig, A. M. (1997) The geochemistry of volatile fluid flow in shear zones. In *Deformation-Enhanced Melt Segregation and Metamorphic Fluid Transport*, ed. M. Holness, pp. 227–266. The Mineralogical Society Series, Chapman and Hall, **8**.

McKenzie, D. P. (1984) The generation and compaction of partially-molten rock. *Journal of Petrology* **25,** 713–765.

McKenzie, D. P. (1985) The extraction of magma from the crust and mantle. *Earth and Planetary Sciences Letters* **74,** 81–91.

Mercier, J. L., Sebrier, M., Lavenu, A., Cabrera, J., Bellier, O., Dumont, J.-F. and Machare, J. (1992) Changes in the tectonic regime above a subduction zone of Andean type: The Andes of Peru and Bolivia during the Pliocene–Pleistocene. *Journal of Geophysical Research* **97,** 11 945–11 982.

Moench, R. H. (1971) *Geologic map of the Rangeley and Phillips quadrangles, Franklin and Oxford Counties, Maine*. U.S. Geological Survey, Miscellaneous Investigations Map, I-605.

Moench, R. H. and Hildreth, C. T. (1976) *Geologic Map of the Rumford Quadrangles, Oxford and Franklin Counties, Maine*. U.S. Geological Survey Quadrangle Map, GQ-1272.

Moench, R. H. and Pankiwskyj, K. A. (1988) *Geologic Map of Western Interior Maine*. U.S. Geological Survey, Miscellaneous Investigations Map, I-1692.

Moench, R. H. and Zartman, R. E. (1976) Chronology and styles of multiple deformation, plutonism, and polymetamorphism in the Merrimack Synclinorium of western Maine. *Geological Society of America Memoir* **146,** 203–238.

Moench, R. H., Boone, G. M., Bothner, W. A., Boudette, E. L., Hatch, N. L., Jr, Hussey, A. M. II, Marvinney, R. G. and Aleinikoff, J. N. (1995) *Geologic map of the Sherbrooke–Lewiston area, Maine, New Hampshire, and Vermont, United states, and Quebec Canada*. U.S. Geological Survey, Miscellaneous Investigations Map I-1898-D.

Nakashima, Y. (1995) Transport model of buoyant metamorphic fluid by hydrofracturing in leaky rock. *Journal of Metamorphic Geology* **13,** 727–736.

Neves, S. P., Vauchez, A. and Archanjo, C. J. (1996) Shear zone-controlled magma emplacement or magma-assisted nucleation of shear zones? Insights from northeast Brazil. *Tectonophysics* **262,** 349–364.

Nyman, M. W. and Karlstrom, K. E. (1997) Pluton emplacement processes and tectonic setting of the 1.42 Ga Signal batholith, SW USA: Important role of crustal anisotropy during regional shortening. *Precambrian Research* **82,** 237–263.

O'Hara, K. D. (1994) Fluid–rock interaction in crustal shear zones: A directed percolation approach. *Geology* **22,** 843–846.

Oliver, N. H. S. (1996) Review and classification of structural controls on fluid flow during regional metamorphism. *Journal of Metamorphic Geology* **14,** 477–492.

Oliver, N. H. S., Cartright, I., Wall, V. J. and Golding, S. D. (1993) The stable isotope signature of kilometer-scale fracture dominated metamorphic fluid pathways, Mary Kathleen, Australia. *Journal of Metamorphic Geology* **11,** 705–720.

Ord, A. (1990) Mechanical controls on dilatant shear zones. In *Deformation Mechanisms, Rheology and Tectonics*, eds R. J. Knipe and E. H. Rutter, pp. 183–192. Geological Society Special Publication, **54**.

Ord, A. and Hobbs, D. E. (1989) Strength of the continental crust, detachment zones and the development of plastic instabilities. *Tectonophysics* **158,** 269–289.

Ord, A. and Oliver, N. H. S. (1997) Mechanical controls on fluid flow during regional metamorphism: some numerical models. *Journal of Metamorphic Geology* **15,** 345–359.

Pankiwskyj, K. A. (1978) Bedrock geology of the Dixfield Quadrangle, Maine. *Maine Geological Survey Open File Map* **78-15,** (scale 1:63500).

Paterson, M. S. (1995) A theory for granular flow accommodated by material transfer via an intergranular fluid. *Tectonophysics* **245,** 135–152.

Paterson, S. R. and Fowler, T. K. J. (1993) Re-examining pluton emplacement processes. *Journal of Structural Geology* **15,** 191–206.

Paterson, S. R. and Miller, R. B. (1998) Magma emplacement during arc-perpendicular contraction. *Tectonics* **17,** 571–586.

Paterson, S. R., Fowler, T. K., Jr and Miller, R. B. (1996) Pluton emplacement in arcs: A crustal-scale exchange process. *Transactions of the Royal Society of Edinburgh: Earth Sciences* **87,** 115–123.

Pattison, D. R. M. and Tracy, R. J. (1991) Phase equilibria and thermobarometry of metapelites. *Reviews in Mineralogy* **26,** 105–206.

Pavlis, T. L. (1996) Fabric development in syn-tectonic intrusive sheets as a consequence of melt-dominated flow and thermal softening of the crust. *Tectonophysics* **253,** 1–31.

Petford, N. (1996) Dykes or diapirs. *Transactions of the Royal Society of Edinburgh: Earth Sciences* **87,** 105–114.

Petford, N., Kerr, R. C. and Lister, J. R. (1993) Dyke transport of granitic magmas. *Geology* **21,** 843–845.

Phillips, W. J. (1972) Hydraulic fracturing and mineralization. *Journal of the Geological Society of London* **128,** 337–359.

Pollard, D. D. and Muller, O. H. (1976) The effect of gradients in regional stress and magma pressure on the form of sheet intrusions in cross section. *Journal of Geophysical Research* **81,** 975–984.

Pressley, R. A. and Brown, M. The Phillips Pluton, Maine, USA: Evidence of Heterogeneous Crustal Sources, and Implications for Granite Ascent and Emplacement Mechanisms in Convergent Orogens *Lithos* (in press).

Price, N. J. and Cosgrove, J. W. (1990) *Analysis of Geological Structures*. Cambridge University Press, Cambridge.

Reches, Z. and Fink, J. (1988) The mechanism of intrusion of the Inyo dyke, Long Valley Caldera, California. *Journal of Geophysical Research* **93,** 4321–4334.

Robin, P.-Y. F. and Cruden, A. R. (1994) Strain and vorticity patterns in ideally ductile transpression zones. *Journal of Structural Geology* **16,** 447–467.

Robin, P.-Y. F. and Cruden, A. R. (1997) *Low Viscosity Shear Zones Within Broader Ductile Transpression Zones. Part I: Analytical Models*. Abstract, Canadian Tectonics Group AGM, Halifax.

Roering, C., van Reenen, D. D., Smit, C. A. and Du Toit, R. (1995) Deep crustal embrittlement and fluid flow during granulite metamorphism in the Limpopo Belt, South Africa. *The Journal of Geology* **103,** 673–686.

Roman-Berdiel, T., Gapais, D. and Brun, J. P. (1995) Analog models of laccolith formation. *Journal of Structural Geology* **17,** 1337–1346.

Rubin, A. M. (1993a) Dykes vs. diapirs in viscoelastic rock. *Earth and Planetary Science Letters* **117,** 653–670.

Rubin, A. M. (1993b) On the thermal viability of dykes leaving magma chambers. *Geophysical Research Letters* **20,** 257–260.

Rubin, A. M. (1993c) Tensile fracture of rock at high confining pressure: Implications for dyke propagation. *Journal of Geophysical Research* **98,** 15 919–15 935.

Rubin, A. M. (1995a) Propagation of magma-filled cracks. *Annual Reviews of Earth and Planetary Science* **23,** 287–336.

Rubin, A. M. (1995b) Getting granite dykes out of the source region. *Journal of Geophysical Research* **100,** 5911–5929.

Rumble, D. (1994) Water circulation in metamorphism. *Journal of Geophysical Research* **99,** 15 499–15 502.

Ruppel, C. and Hodges, K. V. (1994) Pressure–temperature–time paths from two-dimensional thermal models: prograde, retrograde, and inverted metamorphism. *Tectonics* **13,** 17–44.

Rushmer, T. (1995) An experimental deformation study of partially molten amphibolite: Application to low-fraction melt segregation. *Journal of Geophysical Research* **100,** 15 681–15 696.

Rushmer, T. (1996) Melt segregation in the lower crust: How have experiments helped us? *Transactions of the Royal Society of Edinburgh: Earth Sciences* **87,** 73–83.

Rutter, E. H. (1997) The influence of deformation on the extraction of crustal melts: A consideration of the role of melt-assisted granular flow. In *Deformation-Enhanced Melt Segregation and Metamorphic Fluid Transport*, ed. M. Holness, pp. 82–110. The Mineralogical Society Series, Chapman and Hall, London, **8**.

Rutter, E. H. and Neumann, D. H. K. (1995) Experimental deformation of partially molten Westerly granite, with implications for the extraction of granitic magmas. *Journal of Geophysical Research* **100,** 15 696–15 715.

Sawyer, E. W. (1994) Melt segregation in the continental crust. *Geology* **22,** 1019–1022.

Sawyer, E. W. (1996) Melt-segregation and magma flow in migmatites: Implications for the generation of granite magmas. *Transactions of the Royal Society of Edinburgh: Earth Sciences* **87,** 85–94.

Sawyer, E. W. (1998) Formation and evolution of granite magmas during crustal reworking: the significance of diatexites. *Journal of Petrology* **39,** 1147–1167.

Scaillet, B., Pêcher, A., Rochette, P. and Champenois, M. (1995) The Gangotri granite (Garhwal Himalaya): Laccolithic emplacement in an extending collisional belt. *Journal of Geophysical Research* **100,** 585–607.

Scott, D. and Stevenson, D. (1984) Magma solitons. *Geophysical Research Letters* **11,** 1161–1164.

Searle, M. P., Parrish, R. R., Hodges, K. V., Hurford, A., Ayres, M. W. and Whitehouse, M. J. (1997) Shisha Pangma Leucogranite, South Tibetan Himalaya: Field relations, geochemistry, age, origin, and emplacement. *Journal of Geology* **105,** 295–317.

Secor, D. T. (1969) *Mechanics of Natural Extension Fracturing at Depth in the Earth's Crust*. Geological Survey of Canada, Paper 68-52, pp. 3–48.

Secor, D. T. and Pollard, D. (1975) On the stability of open hydraulic fractures in the Earth's crust. *Geophysical Research Letters* **2,** 510–513.

Shea, W. T., Jr and Kronenberg, A. K. (1992) Rheology and deformation mechanisms of an isotropic mica schist. *Journal of Geophysical Research* **97,** 15 201–15 237.

Shea, W. T., Jr and Kronenberg, A. K. (1993) Strength and anisotropy of foliated rocks with varied mica contents. *Journal of Structural Geology* **15,** 1097–1121.

Sibson, R. H. (1974) Frictional constraints on thrust, wrench, and normal faults. *Nature* **249,** 542–544.

Sibson, R. H. (1990) Conditions for fault-valve behavior. In *Deformation Mechanisms, Rheology and Tectonics*, eds R. J. Knipe and E. H. Rutter, Vol. 54, pp. 15–28. Geological Society Special Publication.

Sleep, N. H. (1988) Tapping of melt by veins and dykes. *Journal of Geophysical Research* **93,** 10 255–10 272.

Smith, H. A. and Barreiro, B. (1990) Monazite U–Pb dating of staurolite grade metamorphism in pelitic schists. *Contributions to Mineralogy and Petrology* **105,** 602–615.

Solar, G. S. (1996) Relationship between ductile deformation and granite magma transfer, Tumbledown Mountain area, west-central Maine. In *Guidebook to Field Trips in Northern New Hampshire and Adjacent Regions of Maine and Vermont*, ed. M. R. van Baalen, Vol. 88, pp. 341–362. New England Intercollegiate Geological Conference.

Solar, G. S. and Brown, M. (in press) The classic metamorphism of west-central Maine, U.S.A.: Is it post-tectonic or syn-tectonic? Evidence from porphyroblast-matrix relations. *Canadian Mineralogist*.

Solar, G. S., Pressley, R. A., Brown, M. and Tucker, R. D. (1998) Granite ascent in convergent orogenic belts: testing a model. *Geology* **26,** 711–714.

Spence, D. A., Sharp, P. W. and Turcotte, D. L. (1987) Buoyancy-driven crack propagation: A mechanism for magma migration. *Journal of Fluid Mechanics* **174,** 135–153.

Stephenson, E. L., Maltman, A. J. and Knipe, R. J. (1994) Fluid flow in actively deforming sediments: 'dynamic permeability' in accretionary prisms. In *Geofluids: Origin, Migration and Evolution of Fluids in Sedimentary Basin*, ed. J. Parnell, Vol. 78, pp. 113–125. Geological Society Special Publication.

Stevenson, D. J. (1989) Spontaneous small-scale melt segregation in partial melts undergoing deformation. *Geophysical Research Letters* **16,** 1067–1070.

Stewart, D. B. (1989) Crustal processes in Maine. *American Mineralogist* **74,** 698–714.

Stewart, D. B., Wright, B. E., Unger, J. D., Phillips, J. D. and Hutchinson, D. R. (principal compilers) (1992) *Global Geoscience Transect 8: Quebec–Maine–Gulf of Maine Transect, Southeastern Canada, Northeastern United States of America*, pp. 1–17. U.S. Geological Survey, to accompany map, I-2329.

Terzaghi, K. (1925) *Erdbaumechanic auf Bodenphysikalischer Grundlage*. Franz Deuticke, Vienna.

Thompson, A. B. (1996) Fertility of crustal rocks during anatexis. *Transactions of the Royal Society of Edinburgh: Earth Sciences* **87,** 1–10.

Thompson, A. B. (1997) Flow and focusing of metamorphic fluids. In *Fluid Flow and Transport in Rocks*, eds B. Jamtveit and B. W. D. Yardley, pp. 297–314. Chapman and Hall, London.

Thompson, A. B. and Connolly, J. A. D. (1995) Melting of the continental crust: some thermal and petrological constraints on anatexis in continental collision zones and other tectonic settings. *Journal of Geophysical Research* **100,** 15 565–15 579.

Thompson, A. B., Schulmann, K. and Jezek, J. (1997) Thermal evolution and exhumation in obliquely convergent (transpressive) orogens. *Tectonophysics* **280,** 171–184.

Tikoff, B. and Teyssier, C. (1994) Strain modeling of displacement-field partitioning in transpressional orogens. *Journal of Structural Geology* **11,** 1575–1588.

Tullis, J., Yund, R. and Farver, J. (1996) Deformation-enhanced fluid distribution in feldspar aggregates and implications for ductile shear zones. *Geology* **24,** 63–66.

Turcotte, D. L. and Schubert, G. (1982) *Geodynamics—Applications of Continuum Physics to Geological Problems*. John Wiley & Son, New York.

Unger, J. D., Liberty, L. M., Phillips, J. D. and Wright, B. E. (1989) Creating a 3-dimensional transect of the Earth's crust from craton to ocean basin across the N. Appalachian Orogen. In *3-Dimensional Applications in Geographical Information Systems*, ed. J. Raper, pp. 137–148. Taylor and Francis, London.

Vigneresse, J. L. (1988) Formes et volume des plutons granitiques. *Bulletin de la Société Géologique de France* **8,** 897–906.

Vigneresse, J. L. (1990) Use and misuse of geophysical data to determine the shape at depth of granitic intrusions. *Geological Journal* **25,** 249–260.

Vigneresse, J. L. (1995) Control of granite emplacement by regional deformation. *Tectonophysics* **249,** 173–186.

Walder, J. and Nur, A. (1984) Porosity reduction and crustal pore pressure development. *Journal of Geophysical Research* **89,** 11 539–11 548.

Wang, J. N., Hobbs, B. E., Ord, A., Shimamoto, T. and Toriumi, M. (1994) Newtonian dislocation creep in quartzites: Implications for the rheology of the lower crust. *Science* **265,** 1204–1206.

Warren, R. G. and Ellis, D. J. (1996) Mantle underplating, granite tectonics, and metamorphic *P–T–t* paths. *Geology* **24,** 663–666.

Weertman, J. (1971) Theory of water-filled crevices in glaciers applied to vertical magma transport beneath oceanic ridges. *Journal of Geophysical Research* **76,** 1171–1183.

Weinberg, R. F. (1996) The ascent mechanism of felsic magmas: News and views. *Transactions of the Royal Society of Edinburgh: Earth Sciences* **87,** 95–103.

Weinberg, R. F. (1997) Diapir-driven crustal convection: decompression melting, renewal of the magma source and the origin of nested plutons. *Tectonophysics* **271,** 217–229.

Weinberg, R. R. and Podladchikov, Y. (1994) Diapiric ascent of magmas through power-law crust and mantle. *Journal of Geophysical Research* **99,** 9543–9559.

West, D. P., Jr and Hubbard, M. S. (1997) Progressive localization of deformation during exhumation of a major strike-slip shear zone: Norumbega fault zone, south-central Maine, USA. *Tectonophysics* **273,** 185–201.

Wickham, S. M. (1987) The segregation and emplacement of granitic magmas. *Journal of the Geological Society, London* **144,** 281–297.

Wiggins, C. and Spiegelman, M. (1995) Magma migration and magmatic solitary waves in 3-D. *Geophysical Research Letters* **22,** 1289–1292.

Williamson, K. and Seaman, S. J. (1996) K-feldspar megacrysts, magma mingling, and granitic magma evolution in the Lexington Batholith, west-central Maine. *Geological Society of America, Abstracts with Programs* **28,** A–481.

Wong, T. F., Ko, S.-C. and Olgaard, D. L. (1997) Generation and maintenance of pore pressure excess in a dehydrating system II. Theoretical analysis. *Journal of Geophysical Research* **102,** 841–852.

Zartman, R. E., Hurley, P. M., Krueger, H. W. and Gilletti, B. J. (1970) A Permian disturbance of K–Ar radiometric ages in New England—its occurrence and cause. *Geological Society of America Bulletin* **81,** 3359–3374.

Zen, E-an (1995) Crustal magma generation and low-pressure high-temperature regional metamorphism in an extensional environment; possible application to the Lachlan Belt, Australia. *American Journal of Science* **295,** 851–874.

Zen, E-an, Stewart, D. B. and Fyffe, L. R. (1986) Paleozoic tectonostratigraphic terranes and their boundaries in the mainland northern Appalachians. *Geological Society of America, Abstracts with Programs* **18,** 800.

Zoback, M. L. (1992) First- and second-order patterns of stress in the lithosphere: The world stress map project. *Journal of Geophysical Research* **97,** 11 703–11 728.